STOCHASTIC PETRI NET MODELING
OF
WAVE SEQUENCES IN CARDIAC ARRHYTHMIAS
by
TOSHIO MICHAEL CHIN

Submitted to the Department of Electrical Engineering and Computer Science in March, 1990 in partial fulfillment of the requirements for the Degrees of Master of Science and Electrical Engineer

Abstract

We describe a methodology for modeling heart rhythms observed in electrocardiograms. In particular, we present a procedure to derive simple dynamic models that capture the cardiac mechanisms which control the particular timing sequences of P and R waves characteristic of different arrhythmias. By treating the cardiac electro-physiology at an aggregate level, simple network models of the wave generating system under a variety of diseased conditions can be developed. These network models are then systematically converted to stochastic Petri nets which offer a compact mathematical framework to express the dynamics and statistical variability of the wave generating mechanisms.

Thesis Supervisor:
Dr. Alan S. Willsky, Professor of Electrical Engineering

Acknowledgement

This research was supported in part by the Air Force Office of Scientific Research under Grant AFOSR-82-0258 and by the Harvard-MIT Health Science and Technology Medical Engineering and Medical Physics Fellowship.

Contents

1 Introduction

Monitoring the heart functions through electrocardiograms (ECG's) is practiced so frequently in a variety of medical cases today that there are desires and necessities to automate it in many situations. The ECG's are recordings of electrical events taken over time on body surfaces, and they consist of a series of characteristic spikes, or *waves*, indicative of the electrical and mechanical activities in the heart. Cardiac arrhythmias are conditions where these activities in the heart become abnormally synchronized. Many common cardiac arrhythmias can be detected and classified based solely on the *timing* of various types of ECG waves. To develop a classification algorithm for cardiac arrhythmias, these wave arrival patterns must be represented in a mathematically formal way. The representation must be sophisticated enough to capture a wide variety of wave patterns, yet at the same time it must be simple enough to facilitate formulation of a classification algorithm. This work presents a new methodology for the construction of concise models that accurately capture the wave timing characteristics of a wide variety of cardiac rhythms.

A modeling philosophy

The motivation for this work comes from successes and limitations of previous studies in arrhythmia classification algorithms. Of fundamental importance in the design of such algorithms is the representations and organization of knowledge about cardiac arrhythmias, i.e., modeling. The nature and extent of the models can often dictate such considerations as the tools for decision making, robustness of the resulting algorithm, and the number of classifiable arrhythmias.

One of the most popular approaches in arrhythmia classification is algorithm design based on decesion trees (e.g. [1][15]). Decision trees are flow charts of simple logical rules. At each node of the tree, a logical decision is made based on a specific measurement on the ECG data to narrow the clas-

sification choices. As the decision making process moves along a branch of the tree, necessary additional measurements on the ECG are specified to ultimately choose a single arrhythmia class. Decision making based on a series of deterministic logical rules, however, has a fundamental difficulty in dealing with uncertainties. For example, a "border line case" at a decision node or noise in the data can lead the process to go down along a wrong branch of the tree. A great deal of effort has been spent to make the decision logic robust against conceivable sources of uncertainty, at the cost of greatly increasing complexity of the trees. Another important factor contributing to the complexity of decision trees is the complexity of the cardiac arrhythmia phenomena themselves. Many arrhythmias must be classified based on *trends* over several heart beats; moreover, variations within a single class of arrhythmia are quite common.

This work is concerned with capturing, in a unified modeling framework, the behavior of ECG wave sequences under various arrhythmic conditions. Specifically, we present a stochastic Petri net implementation of a *dynamic* representation of electrophysiological *mechanisms* which are responsible for arrhythmic wave sequences. That is, the models presented here are (i)physiological and (ii)probabilistic:

Physiological v.s. phenomenological

In a sense, the decision trees mentioned above imply *phenomenological* models of cardiac arrhythmias as each arrhythmia class is "defined" by a set of logical rules in the decision nodes. It is phenomenological because arrhythmia classes are characterized *directly* by observable features on ECG. Such models cannot avoid being complex, as phenomena seen in arrhythmic ECG's are complex. The model complexity is only increased further when more sophisticated decision rules are introduced to deal with uncertainties. These additional decision rules can easily blur the original descriptions of the arrhythmia classes. Alternatively, one can explicitly model the cardiac mechanisms responsible for the generation of arrhythmic ECG waves, because a variety of arrhythmias can be explained coherently in a single framework of cardiac electrophysiology. One

of the purposes of this work is to demonstrate that by identifying and modeling some macroscopic electrical events in the heart one can describe many common cardiac arrhythmias coherently and concisely.

Probabilistic v.s. deterministic

One advantage of probabilistic models over deterministic ones is that uncertainties in data (e.g. noise) and in decision making (e.g. multiple candidates) are more naturally represented in a probabilistic setting. In addition, for the specific models presented in this work, we need to characterize some macroscopic electrophysiological events in the heart. Each of these events is a result of electrical activities in an ensemble of cardiac muscle cells. Probabilistic models are suited for characterizing collective effects such as this.

Previous work: Probabilistic arrhythmia models

In the past, relatively simple Markov (i.e., probabilistic) models were used to describe a small number of cardiac arrythmia classes, and classification algorithms were developed based on these models. For example, in the work by Gersch *et al.*[3] each of six chosen arrhythmia classes was modeled by a three-state Markov chain. The states of the chain represent "regular", "short", and "long" intervals between successive heart beats which can be measured from the most prominent ECG features, the R waves. The transition probabilities of the chains were determined based on the appropriate statistics from a learning set of ECG data corresponding to the six arrhythmia classes. To classify observed ECG data, the algorithm first takes transitional statistics of intervals between successive R waves (e.g., how often is a "regular" interval followed by a "short"?) and then evaluates which of the six Markov chains is the most likely to produce such statistics.

One problem associated with such an arrhythmia classification algorithm is that the observed R wave (i.e., heart beat) intervals must be arbitrarily classified as regular, short, or long. This is a practical disadvantage because of individual variations in the heart rate. The classification algorithm developed by Gustafson *et al.*[4] avoids this particular problem. In this algorithm, the R

wave intervals are modeled as the output of a linear time-invariant dynamic system. Four such dynamic models are presented in [4] to model four chosen arrhythmia classes. To classify an observed R wave interval sequence, the Kalman filter corresponding to each dynamic model produces a tracking error sequence[1]. The probability distributions of the error sequence in the ideal case, i.e, when the statistical properties of the observation match perfectly with that of the model output, are known, and such distributions are used to compute the likelihood that the observation matches with each dynamic model. As presented in [4], computation of the likelihoods can be performed sequentially, and with some additional sophistication in the dynamic models, one can develop an algorithm not only to classify arrhythmias but also to detect the onsets of changes from one class to another in the ECG observation.

Previous work: Physiological arrhythmia models

The use of simple Markov models by Gersch *et al.*[3] and Gustafson *et al.*[4] has led to the development of arrhythmia classification algorithms which are computationally elegant and statistically optimal (i.e., the "best choice" is mathmatically well-defined). The major limitation is, however, that such models are appropriate for a limited class of arrhythmias. For example, none of these Markov models has been extended successfully to accommodate the observations of the P waves, less prominent than the R waves yet essential in the characterization of many cardiac arrhythmias[5]. The problem is that the state space for complex wave sequences of cardiac arrhythmias cannot be easily identified phenomenologically.

Doerschuk[2] has demonstrated, however, that Markovian description of such wave sequences are nevertheless possible by modeling the physiological mechanisms responsible for the wave sequences. Each of Doerschuk's models consists of several interacting Markov chains, and each of these Markov chains describes the electrical activities in major components of the electrical conduction system in the heart. These Markov chains "interact" with each

[1] also called a *residual* or *innovation* sequence in the literature

other in such a way that the state of one chain can alter the transition probabilities of another chain. Such "interacting Markov chain" arrangements are motivated both by physiological facts and practical considerations. Namely, as described in the sequel, the interactions between major components of the cardiac electrical conduction system occur relatively infrequently and usually have some deterministic effects. In another words, the electrical activities in these components are independent of each other *most of the time*, and it is not unreasonable that they are modeled by separate (but interacting) Markov chains. A practical advantage of the "interacting Markov chain" representation over the full enumeration of the corresponding state space (i.e., a single, large Markov chain) is that the former is more compact and descriptive, making model development, interpretation, and analysis more manageable.

Towards stochastic Petri net modeling

Conceptually, one can imagine developing a arrhythmia classification algorithm based on the "interacting Markov chain" model[2] by (i)builing a model for each arrhythmia class, (ii)expand each of these model into a single Markov chain, and (iii)compute the likelihood that each Markov chain generates the observed ECG wave sequence. Although steps (ii) and (iii) are identical to the setup for the previously mentioned algorithm by Gersch *et al.*[3], the Markov chain in (ii) is too large for such an algorithm to be computationally feasible. Instead, Doerschuk[2] developed a suboptimal classification algorithm by approximating parts of his "interacting Markov chain" by simpler Markov chains[2]. Namely, to evaluate the likelihood that a model has generated the observed ECG wave sequence, the most likely state trajectories in the Markov chains in the model must be computed using sparse observations of state trajectories. The suboptimal state trajectory estimator described in [2] is essentially an iterative improvement scheme where at each step the optimal state trajectory at one of the Markov chains is computed under the assumption that the interactions from other Markov chains can be described by the behavior of much simpler (e.g., two states) chains. The iteration continues at

least while such *locally* optimal state trajectories are computed once for all Markov chains. Despite its potentials, this suboptimal algorithm has not been completely implemented due to its complexity.

From the perspective of developing such an arrhythmia classification algorithm, it is apparent that a more compact representation than Markov chains is desirable to facilitate description (approximate or otherwise) of the behaviors of the interacting model components. A shortcoming of the "interacting Markov chain" models is, in fact, their complexity due to the nature of the representations used. In particular, the desire to use Markov chains, i.e., desire to directly construct a state description, forces one to deal simultaneously with fine-level timing parameters and more aggregate structural aspects of the model. Because of this, some of the conciseness of description desirable for not only algorithm design but also model construction is lost.

This work was motivated by the belief that stochastic Petri nets are more suitable for concise modeling of the cardiac electrical events. In particular, in this framework one can quite easily separate and control the two significant aspects of cardiac activity highlighted in Doerschuk's model – namely the *timing* of events in different parts of the heart and the *interactions* among these parts. As we will see, the interactions specify the complete structure of the Petri net model, while timing information affects specific parameter values within the structure.

This thesis is organized as follows: In Section 2 we review those aspects of cardiac electro-physiology of importance for the modeling of ECG rhythms. We place particular emphasis on the mechanisms generating sequences of P and R waves. We then represent these mechanisms as dynamic systems containing concurrently operating, stochastic, timing processes. In Section 3, stochastic Petri nets are introduced. As this modeling formalism was expressly developed to model concurrently operating and interacting processes, it is a natural choice for modeling cardiac rhythm. In Section 4 we show how the flow models developed in Section 2 can be transformed into dynamic models of the type described in Section 3. In particular, a systematic procedure to generate

stochastic Petri net models of various cardiac arrhythmias is described. We illustrate the procedure through the construction and simulation of models for several different cardiac arrhythmias. Finally, Section 5 concludes the thesis with a summary of the work and discussion of possible extensions.

2 The Cardiac Electrical Conduction System

In this section we identify and categorize various electrical events in the heart in order to facilitate modeling of cardiac arrhythmias. We describe three important features of the cardiac electro-physiology: autorhythmic rate, conduction delay, and refractory period. Based on these three we then define the basic subunits of the electrical conduction system in the heart — rhythm and transmission elements. We show that various common cardiac arrhythmias can be dynamically characterized by networks of these rhythm and transmission elements.

2.1 Electrical Activity in the Heart Cells

General characteristics of the electrically active cells in the heart have been well studied and documented. The following is a brief summary of those characteristics important in explaining the mechanisms of many common cardiac arrhythmias. For more details see, for example, [8] and [13].

The ECG is a recording of the net electrical potential difference produced when the cardiac muscle cells are excited electrically. All cardiac muscle cells follow the same electrical excitation pattern: At rest, they maintain a certain voltage (about -90 mV) across the cell membrane. But if a sudden change in the electrical environment of the cell raises the cross-membrane voltage above a certain threshold, then the cell reacts to increase the voltage spontaneously to a higher level (about 10 mV). This spontaneous, quick increase in cross-membrane voltage is the onset of the excitation.[2] The voltage soon falls back to the original resting level (thus forming an electrical pulse). However, it takes the cells a little longer to return to the same excitable state. During this period the cells cannot be induced to increase their cross-membrane voltages spontaneously, and this duration is called the *refractory period.* The cardiac muscle cells come out of the refractory period in about 300 miliseconds after

[2]This phenomenon, observed also in nerve cells and skeletal muscle cells, is called *depolarization.*

the onset of the excitation, at which time they become ready for another excitation.

Most commonly, electrical excitations in a cardiac muscle cell are triggered by excitations in its neighboring cells.[3] For example, if a section of a muscle tissue from the heart is electrically stimulated, the excitation spreads quickly into the entire tissue. In such inter-cellular transmission of electrical excitation, the refractory period is important because it prevents back-flows and reflections. For example, suppose that the excitation of cell A triggers excitation in cell B, a neighbor. Since cell A will be in refractory period, cell B will not be able to transmit the same excitation back to cell A. But suppose that cell B has a neighbor cell C which is not a neighbor of cell A and is ready to be excited. Then cell B can transmit the excitation to cell C. The refractory period, thus, gives directionality in inter-cellular transmission of electrical excitation.

As described above, most cardiac muscle cells are induced into activity by receiving excitation from neighboring cells. However, many cardiac muscle cells also have a mechanism to generate periodic excitations by themselves. In fact, the cross-membrane voltage in these cells at rest rises slowly towards the threshold for the spontaneous, quick increase that characterizes the excitation of the cells. This property is called *autorhythmicity.* The rate at which the resting voltage reaches the excitation threshold differs from cell to cell. The heart has a collection of cells which have the fastest of such rates and specialize in the generation of periodic excitations. In a normal heart, the cells in a region, called the *SA node* on the wall of the right atria are the source of these excitations. The periodic electrical activity of the SA node is eventually transmitted throughout the heart, and the muscle cells of the atria and ventricles contract, just as all skeletal muscle cells do, upon reception of the electrical excitation. The rate at which the SA node excites is, thus, observed as the heart rate in a normal heart.

[3]This is accomplished through the *gap junctions*, cross-cellular channels for intra-cellular plasma. Increase in electrical potential inside a cell causes the potentials inside its neighbor cells to rise.

2.2 Normal Heart Activity and the Electrocardiogram

The heart consists of two pairs of chambers: the *atria* and *ventricles*. The two pairs contract alternately in such a fashion that the atria pump blood from the veins into the ventricles which then pump it to the lung and the rest of the body. At contraction, an electrical excitation is transmitted quickly throughout the muscle cells of the chamber pair. This nearly-simultaneous excitation of many cells is observed as a peak on the ECG recording. Because the ventricles have much larger muscle mass than the atria, they produce a conspicuous peak called the *R wave*[4], while the atria produce a small (and often difficult to detect) peak called the *P wave*. The timing of chamber contractions is orchestrated by a network of muscle cells specialized in generation and transmission of electrical excitations. The electrical activities in a normal heart are as follows: The SA node generates excitations periodically due to its autorhythmicity[5]. These excitations spread throughout the atria, inducing contractions. They also reach the *AV node* on the wall separating the atria from the ventricles. The AV node is the only normal electrical channel between the two pairs of heart chambers, and its excitation is normally transmitted to the muscle cells of the ventricles through specialized conducting muscle cells called the *Purkinje fibers*. Unlike intra-muscluar conduction, the transmission of electrical excitation through the AV node is slow. In effect, this delays contraction of the ventricles from that of the atria, so that the blood can flow in the correct direction from the atria to ventricles. The delay through the AV node, thus, plays an important role in the control of chamber contraction.

In rhythm analysis of the ECG, we try to make an assessment on how well this electrical conduction system is controlling chamber contraction. The intervals between P and R waves are studied for this purpose. In many diseases, parts of the cardiac electrical conduction system are affected, and we observe distinct, anomalous patterns in P,R wave sequences. These known patterns

[4]Strictly speaking this should be the *QRS complex*, a sequence of three waves. But for simplicity, we use the term "R wave" to refer to the ECG feature corresponding to the contraction of the ventricles.

[5]The autorhythmic rate of the SA node is under autonomic nervous control.

form a very important diagnostic basis for cardiac arrhythmias.

2.3 Control of the Cardiac Electrical Conduction System

The electrical conduction system of the heart has two main functions: generation of electrical excitations and distribution of these throughout the heart. Generally speaking, these functions are regulated by three timing parameters: autorhythmic rate, conduction delay, and refractory period. This subsection describes how these timing parameters affect the functions of the system. 1)Autorhythmic rate. Normally, the SA node has the fastest autorhythmic rate in the whole system, and the heart activities are paced at this rate. However, non-SA nodal tissue can sometimes attain an autorhythmic rate comparable to that of the SA node. In such a system, two or more rhythm sources compete to pace the heart, resulting in an anomalous and possibly chaotic contraction pattern. This phenomenon can occur either when the rate at the SA node slows down abnormally or, more commonly, when the rate of non-SA nodal tissue speeds up drastically. 2)Conduction delay. As mentioned before, the conduction speed through the AV node has an important function in delaying ventricular contractions after the preceding atrial contractions. This is an example of the direct influence that conduction delays generally have over cardiac control. 3)Refractory period. An abnormally long refractory period can periodically block excitations. For example, suppose that the duration from the onset of excitation to the end of the refractory period at the AV node is slightly longer than the period of autorhythmic excitations at the SA node. The first excitation from the SA node can successfully excite the AV node. The second excitation, however, arrives at the AV node during the refractory period, and it is blocked from propagating further. The resulting P,R sequence in this hypothetical case is a series of P waves alternatingly followed by R waves. In reality, blockage of excitation by the refractory periods is not absolute. In general, the refractory period is loosely divided into two parts. The early part is where excitation is blocked with certainty and is called the

absolute refractory period. In the latter part, the tissue goes through a period where it becomes increasingly prone to be excited, and this period is called the *relative refractory period.* Forcing tissues to excite during their relative refractory period often alters their autorhythmic and trasmission characteristics momentally. For example, an excitation arriving at the AV node during its relative refractory period will take longer than usual to propagate through the node. Also, if a pacing tissue like the SA node for some reason receives an excitation during a relative refractory period, its autorhythmic generation of the next excitation pulse is momentally delayed. Such brief interference with natural autorhythmicity is referred to as either the *resetting* or *stunning* phenomenon. In resetting, the time interval between the reception of the external excitation and the generation of the next autorhythmic excitation is roughly equal to the period of the autorhythmicity. In stunning, on the other hand, this time interval is significantly longer than the period of the autorhythmicity.

2.4 The Rhythm and Transmission Elements

Since the two main functions of the cardiac electrical conduction system are generation and distrubution of electrical excitations, the dynamics of the system can be described by a network of two types of elements. One of these is the *rhythm element*, which generates electrical excitations, and the other is the *transmission element*, which distributs excitation from one section of the system to another. The controlling mechanisms for macroscopic flows of electrical signals (excitations) in the heart can be represented by a network of rhythm and transmission elements. In the next subsection, we represent the dynamics of several cardiac arrhythmias with such networks. In this subsection the two elements are described.

We represent rhythm elements diagramatically as triangles and transmission elements as rectangles (Fig. 1). The rhythm elements are used to describe the autorhythmic properties of cardiac muscle tissues: their primary function is periodic generation of electrical signals. Associated with a rhythm element are input and output terminals as well as several parametric variables that

control the intervals of signal generation. The purposes of these terminals and parameters are as follows: (i)output. The signal generated by the element is sent to neighboring elements through the output terminal. (ii)input. The autorhythmic cells can be stimulated by excitations in neighboring cells. The rhythm element receives such external stimulation through the input terminal. (iii)variables. The fundamental parameter of a rhythm element is the *period* at which it generates signals. However, this basic period can be altered especially when an external stimulation arrives through the input terminal. Thus, besides the basic period, variables that quantitatively characterize the external influence on the function of the element are needed. For example, one such variable is the *refractory period.* Others, associated with such phenomena as resetting and stunning, will be described in Section 4.

The transmission elements are used to describe the delay of signals traveling through cardiac muscle tissues. It is basically a bi-dirctional channel characterized by two pairs of input and output terminals. Signals can be transmitted through the element in either direction, but when two opposing signals meet in the element they annihilate each other. The variables associated with the transmission elements are the *transmission delays* for both directions, *refractory periods* which characterize the excitability of the two input terminals, and other parameteric variables representing the factors that may influence the durations of transmission delays and/or refractory periods. (We will show an example of such factors later when we describe the Wenckebach phenomenon.)

The rhythm and transmission elements are used quite flexiblly, and in particular, the numbers and types of the terminals and variables assigned to an element are adjustable. For example, a uni-directional transmission element would graphically be presented as a rectangle just like a bi-directional transmission element(Fig. 1b) but without the second pair of input and output terminals. Such variations among rhythm and transmission elements are presented in more details in Section 4, when we discuss the implementation of these elements with stochastic Petri nets.

2.5 Signal Flow Block Diagrams

The rhythm and transmission elements described in the preceding subsection allow us to model the timings of P and R waves and aberrancies of different rhythms at a relatively aggregate level. While it is certainly possible to use the modeling methodology developed in this paper to describe cardiac activity at a more detailed level (by partitioning the heart into a larger number of interacting rhythmic and conductive units, each representing a smaller portion of cardiac electrical pathways), the explicit use to which we put this methodology here is at the other extreme. Specifically, by highlighting the mechanism causing and driving particular arrhythmias, we want to obtain the simplest possible models capturing characteristics of the corresponding P,R sequences. Such "minimal representations" should ultimately be of most value as the basis for robust signal processing and automated diagnosis of cardiac arrhythmias.

To illustrate this philosophy, consider the modeling of a perfectly normal heartbeat sequence. We can divide the cardiac condution system into five stages based on their structural and functional differences — the SA node, intra-atrial conductive paths, AV node, Purkinje fiber conductive paths, and ventricles. Each tissue block can in fact excite autorhythmically, and all except the SA node and ventricles (which are the two ends of this electrical system) can conduct bi-directionally. As far as the modeling of a normal P,R sequence is concerned, however, bi-directional conduction is an unnecessary physiological detail since excitations conducting in the retrograde direction (i.e., direction towards the SA node, opposite to the normal direction of the flow of excitation) are never observed in such a sequence. Thus, a model constructed with uni-directional transmission elements instead of bi-directional elements is simpler yet phenomenologically just as acurate. Such a signal flow block diagram model is shown in Figure 2a. The rhythm element representing the SA node does not have an input terminal because of the absence of retrograde-conducting excitation. The autorhythmic excitations of the SA node activate the atria and generate the P waves. The letter "P" by the output terminal represents the generation of the P wave. The excitation also bifur-

cates to activate the trasmission element and reset the rhythm element of the intra-atrial pathways. The excitation produced by the intra-atrial pathways is the result of either the transmission of the excitation originated in the SA node or its own autorhythmic activation. This is represented by the convergence of the outputs of the transmission and rhythm elements. The AV node and Purkinje fibers are reprsented by a parallel pair of transmission and rhythm elements, just like the intra-atrial pathways. The only differences among these three parts of the block diagram are the values of the parameters assigned to the respective transmission and rhythm elements (i.e., conduction delays, autorhythmic intervals, and absolute refractory periods). The output of the Purkinje fibers is directed to the ventricles whose activation produce the R waves. The letter "R" by the input of the ventricles represents the production of the waves. This block diagram model implies that the autorhythmic period of the ventricles is larger than those of other parts of the heart (in particular the SA node) so that the ventricles are "reset" frequently enough not to excite autorhythmically. In the model, therefore, the rhythm element representing the ventricles does not have an output terminal. This is consistent with the assumption that retrograde conduction is absent.

This block diagram model of the normal heart can be simplified further as follows: First, since in a normal cardiac sequence the autorhythmic rate in the SA node is the fastest and drives the entire system, the rhythm elements in the rest of the system are always "reset" before they can generate an autorhythmic excitation. We can, therefore, delete the three rhythm elements used to model the autorhythmic properties of the intra-atrial pathways, AV node, and Purkinje fibers. After these three rhythm elements are removed, the three remaining stages that separate the two wave generators collectively form only a series of three transmission elements. These transmission elements are, thus, combined into one aggregate element, which we call the "AV node" for simplicity. The simplified model of the normal heart is shown in Figure 2b, which has only two rhythm elements and one transmission element.

2.6 Modeling of Common Arrhythmic ECG Patterns

In this subsection, we represent the dynamics of several common cardiac arrhythmias using signal flow block diagrams made up of rhythm and transmission elements. Many of the common arrhythmias are included in the four categories described in this subsection, and Figures 3a to 8a show signal flow models of several examples from each category. Also, to illustrate the wave patterns for these examples of arrhythmias, Figure 3b to 8b present the P,R wave sequences obtained from simulations of the models (See Section 4 for details). P waves are represented by short vertical lines and R waves by long vertical lines, and abnormal waves are represented by lines with small squares at their tips. The interval of time ticks is one second. See [6] for more detailed descriptions of cardiac arrhythmias.

1. Extrasystole – ectopic beat

(i)phenomenology. In this condition, non-SA nodal tissue becomes, either continuously or sporadically, a pacemaker for the heart. Such abnormal pacemakers are called *ectopic* rhythm sources. Ectopic beats may originate in the atrial wall outside the SA node causing untimely atrial contractions and abnormally shaped P waves. This class of cardiac arrhythmia is called *Atrial Premature Beat*, or APB. Ectopic beats may also arise in the AV node, in the Purkinje fibers, or in the ventricular musculature, and they tend to cause *Ventricular Premature Beat*, or VPB. These ectopic beats, in addition, may initiate excitations that flow backward into the atria (i.e., retrograde conduction). The resulting atrial electrical activity is referred to as the *retrograde P wave.* As mentioned before, the SA node can be "reset" or "stunned" by retrograde excitations. *(ii)modeling.* Ectopic beats are caused by abnormally fast autorhythmic rates at non-SA nodal tissues. Rhythm elements are used to represent such ectopic sources. *(iii)examples.* Figures 3a and 4a show examples of signal flow block diagrams of APB and VPB, respectively. Both models consist of three stages – the atria, AV nodes and ventricles – just like the normal heart model in the previous subsection. In the VPB model (Fig. 3a) the atrial stage has two rhythm elements, one for the normal SA nodal beats

and the other for the atrial ectopic beats. The output of each rhythm element resets the other rhythm element and activates the transmission element representing the AV node. The rest of the model is identical to the normal heart described before. The P waves produced by atrial ectopic beats usually have abnormal shapes; in the model a "P" with an overbar denotes that the output of the rhythm element representing the ectopic source generates such abnormal P waves. In the VPB model(Fig. 4a) the ectopic source is generally thought to be in the ventricular tissue. Thus, the rhythm element representing the ventricles has an output terminal whose activation produces a premature, abnormally shaped R wave (denoted by an "R" with an overbar in the figure). Since the excitation generated by the ventricles conducts in the retrograde direction towards the atria, a bi-dirctional transmission element is used to represent the AV node. Retrograde activation of the atria causes a retrograde P wave ("P" with an overbar) and resets the SA nodal autorhythmic source.

2. Extrasystole – coupled beat

(i)phenomenology. This category of cardiac arrhythmias also deals with premature waves. Although the occurence of premature waves in the previous category seem independent from the timing of the normal waves (thus they are thought to be caused by ectopic rhythm sources acting independently from the SA nodal source), the premature waves in this category show some correlation with the SA nodal beats. Specifically, these premature waves are synchronized with the normal beats, and the intervals between premature waves and preceding normal waves are fairly constant. Such intervals are called the *coupling intervals. (ii)modeling.* Although there are several physiological or anatomical explanations for the origin of the coupling intervals, a convenient way to describe the phenomenon is to use a hypothetical electrical conduction channel called the *reentrant pathway.* Conceptually, the reentrant pathway resides within the muscular wall of a heart chamber. It has a conduction delay whose value is equal to that of the coupling interval. It receives an excitation when the chamber is excited to contract, delays the excitation for the amount of the time specified by its conduction delay parameter, and then returns the

excitation back to the chamber. This leads to a second, abnormal contraction of the chamber (and generation of an associated ECG wave) following the normal contraction arising from the direct excitation pathway. In the block diagram, the coupling intervals are described by uni-directional trasmission elements representing the reentrant pathways. *(iii)example.* Figure 5a shows the block diagram for a condition called *bigeminy*, where a premature ventricular contraction occurs every other beat. The first two stages of the model – the SA and AV nodes – are the same as the normal heart. The output of the AV node activates both the ventricles (producing the normal R wave) and the reentrant pathway. The reentrant pathway delays the excitation and activates the ventricles (producing the abnormal R wave). The interval between the normal and succeeding abnormal R waves is the coupling interval in this case, and it is modeled by the delay parameter of the transmission element representing the reentrant pathway. The normal conduction wave (initiated by the SA node) immediately following the premature R wave arrives at the ventricle during its absolute refractory period. Thus, the normal excitation is blocked, and the corresponding R wave is not produced. This is observed as the relatively long interval between a premature R wave and the succeeding normal R wave(Fig. 5b).

3. AV Conduction Block

(i)phenomenology. This category includes arrhythmias caused by abnormalities in conduction between the atria and ventricles. In a complete blockage, called *third degree AV block*, the AV node is entirely unable to conduct excitations. Thus, the contractions of the ventricles must be paced by the autorhythmicity of the AV node, Purkinje fibers, or ventricular musculature itself.[6] The resulting P,R wave sequence displays a case of *AV dissociation*, a phenomenon in which the rhythm of the R waves is independent from that of the P waves. In *second degree AV block*, not all the atrial excitations are blocked by the AV node. When only two out of three P waves are followed by R waves, the condition is referred to as 3:2 block. Other ratios commonly seen are 2:1, 3:1,

[6]This is an example of autorhythmic beats from a non-SA nodal tissue preventing a complete failure of the heart, and these beats are called the *escape beats*.

4:1, and so on. A P,R sequence in this subcategory may also exhibit a *Wenckebach phenomenon* described as follows: The SA node generates excitations at a constant rate, but the P-R interval grows progressively longer during several beats until there is a P wave not followed by an R wave (i.e., a block has occurred). The next P wave is followed by an R wave with a normal, short P-R interval; then, the interval again grows progressively longer over the next several beats as the pattern is repeated. Figure 7b shows an example of a P,R sequence displaying the Wenckebach phenomenon. Finally, in *first degree AV block*, no R wave is missed after any P wave, but the P-R interval is abnormally prolonged. *(ii)modeling.* AV conduction blocks are caused by various disease conditions inside the AV node. Since all the abnormalities occur within the transmission element representing the AV node, the signal flow block diagram is essentially the same as that of the normal heart (Fig. 2b). The transmission element (the AV node), however, tends to have a considerably more complex role than in the normal P,R sequence. (Modeling of the third degree AV block is an exception and is trivially simple; it can be accomplished by removing the transmission element from the normal heart model.) *(iii)examples.* Figure 6a shows a model of second degree AV block. Note that the trasmission element has an extra parameter called "probability of conduction." In 3:2 block, for example, this probability is set to $\frac{2}{3}$. Figure 7a shows a model featuring the Wenckebach phenomenon. A completely different transmission element must be used to describe the dynamics of the AV node. In Wenckebach, events in the current beat are dependent on the events in the previous beats. For example, every P-R interval must be longer than the previous interval unless the R wave is missing from the previous beat; if the R wave is missed the P-R interval must become short again. The transmission element, therefore, must have a "memory" of its actions in the previous beats to determine how it behaves in the current beat. This requires us to describe the transmission element itself as a dynamic system. Detailed specification of the behavior of such a transmission element is discussed in Section 4 in which we describe the implementation of the dynamics of various rhythm and transmission elements.

4. Abnormal conduction path

(i)phenomenon. In a normal heart, electrical insulation exists between the atria and ventricles, and the AV node is the only electrical channel between the pairs of chambers. Some abnormal hearts, however, have conduction pathways that bypass the AV node. For example, in a condition called the Wolff-Parkinson-White syndrome the ECG displays an abnormally early onset of the ventricular activity. It also exhibits broadened R waves because each beat reaches the ventricles through the abnormal and normal (AV nodal) routes and excites different parts of the chambers at slightly different times. *(ii)modeling.* An abnormal conduction channel is represented by a transmission element. *(iii)example.* Figure 8a shows a model of the Wolff-Parkinson-White syndrome. The ventricles are divided into two parts. One of these is excited normally and produces R waves. The other part is excited via the abnormal conduction channel[7] and produces characteristic *delta waves*[8]. The output of the SA node simultaneously activates the normal and abnormal channels. The conduction delay through the abnormal channel is slightly shorter than that through the normal, AV nodal channel. To increase the anatomical accuracy of the model, the two rhythm elements representing the two parts of the ventricles may be connected with a bi-directional transmission element. But since the two parts of the ventricles excite at about the same time, such a transmission element would host only collision and annihilation of two excitations flowing in the opposite directions. This activity does not influence the P,R wave sequence produced by the model. The bi-directional transmission element is, therefore, omitted in favor of model simplicity.

In the preceeding description of the cardiac electrical conduction system, we have identified several of its dynamic properties which enable us to characterize the P,R wave sequences of the cardiac arrhythmias. In the following sections, we describe such dynamics in a mathematically formal way by

[7]called the *bundle of Kent*

[8]The R and delta waves are actually parts of a single peak. The delta wave is identifiable as an abnormally smeared leading edge of the conspicuous R wave peak.

implementing the signal flow block diagrams developed in this section using stochastic Petri nets. This process is similar to translating flow-charts into computer codes using a particular programming language. It is desireable that the programming language has features that allow a straightforward representation of the sequential behavior characterized by the flow-chart. In this context, two important features of the signal flow block diagrams for cardiac arrhythmias should be noted: One is that the system dynamics are regulated by timing parameters, and the other is the concurrency of the dynamics (e.g., the SA node is in its refractory period while the AV node is conducting excitation). In other words, using the block diagrams introduced in this section we have characterized the mechanisms of various cardiac arrhythmias as *concurrent timing processes.* Stochastic Petri nets, which are described in the next section, have been developed to model dynamics of such concurrent timing processes. They, therefore, offer a natural framework for the translation process discussed above.

3 Stochastic Petri Nets

In the preceding section we have seen that the electrical activities of various parts of the heart are governed by local timing parameters such as autorhythmic periods, conduction delays, and refractory periods. These activities interact with each other by passing and receiving excitations, collectively defining the electrical phenomena observed as ECG's. Thus, behaviors of the cardiac electrical conduction system can be considered as a collection of concurrently operating timing processes. Stochastic Petri nets offer a general and flexible format to express the activities of concurrent timing processes. Historically, stochastic Petri nets were developed as the result of an extension of the original Petri net theory which features simpler execution policies (i.e., dynamics). In this section we first review the main features of the original Petri nets before discussing those of stochastic Petri nets. The section closes with a discussion of features of stochastic Petri nets desirable for the modeling of the cardiac electrical conduction system.

3.1 Petri Nets

Petri nets are abstract models of information flow, and they are particularly useful in describing and analyzing the flow of information and control in systems which exhibit asynchronous and concurrent activities. In this subsection, we try to highlight some fundamental properties of Petri nets. Refer to Peterson[10][11] for more detailed discussions of them.

Structure. Petri nets are commonly represented pictorally as directed graphs. Figure 9 shows an example of a Petri net. There are four structual components — two types of nodes, called *places* and *transitions*, and two types of directed arcs, *input* and *output arcs*. A place is represented by a circle ("p0" to "p6" in Fig. 9) and a transition by a bar ("t0" to "t5"). All the directed arcs in a Petri net connect a node of one type with a node of the other type; no arc connects two nodes of the same type. An arc going from a place to a transition is referred to as either an output arc of the place or an input arc

of the transition. Similarly, an arc going from a transition to a place is called either an output arc of the transition or an input arc of the place.

Dynamics. The dynamics of Petri nets are represented by the positions and movements of markers called *tokens*. Tokens are pictorally represented by dots inside places. In the example (Fig. 9), each of the places p0, p2, and p6 has a single token. Tokens can be moved to other places along directed arcs by *firing* transitions on the arcs. A transition can fire only if it is *enabled*. A transition becomes enabled when all its input arcs are connected to places possessing tokens. In the example, t1 and t2 are enabled, and t3 is not enabled because p3 does not have a token.

Decision Rules. Note that in the preceding example t1 and t2 cannot fire at the same time because firing one of them takes the token out of p0 and disables the other. Those transitions competing for the same token(s) are described to be "in conflict." Policies, called the *decision rules*, to resolve such conflicts are thus specified. One implementation of the decision rule is a probabilistic policy. For example, in Figure 9 we can make t2 fire with probability of 0.7 whenever t1 and t2 are in conflict. Note that when this probability is set to 1.0 the decision rule can be considered to be a preferential policy, i.e., t1 can fire only when it is not in conflict with t2 (equivalent to saying that t1 can fire only when p3 has no token). It is clear from this example that the dynamics of some Petri nets cannot be made explicit without decision rules. Once the static properties of a Petri net, i.e., the net topology and initial token placement, are defined, transitions that may potentially be in conflict with each other can be identified. A set of such transitions is called a *conflict set*. Given a Petri net topology and initial token placement, it is important to identify all conflict sets and assign a decision rule for each set. See references [9][12][14] for more detailed discussion on net topology and conflict sets.

To summarize, the dynamics of a Petri net depends on specification of the net structure (topology), the initial placement of the tokens, and the decision rules (if there are conflict sets).

3.2 Stochastic Petri Nets

The original Petri nets, as described above, are defined without the notion of time; however, in *timed Petri nets* some explicitly defined timing parameters ("processing times") influence the evolution of the state of the nets. *Stochastic Petri nets* (SPN's) are those timed Petri nets in which the processing times are specified probabilistically via distribution functions. Indeed, the relation between SPN's and the original, untimed Petri nets is analogous to that between semi-Markov chains and Markov chains. Different versions of SPN's exist. For example, SPN's can be divided into two groups depending on whether the processing times are associated with transitions or places[9]. This issue is particularly important in modeling of cardiac arrhythmias, and we discuss it in detail in this subsection. Another source of diversification of SPN's is the relationship between clocking of the processing times and firing of the tokens. Reference [7] describes various "firing policies" that result because of different interpretations of this relationship. The firing policy of interest in this paper is called the "race" policy which is assumed in the descriptions below.

Transition-timed SPN. In transition-timed SPN's, the processing times are associated with transitions. When a transition is enabled, a sample of the random variable representing the corresponding processing time is chosen, and the transition must wait for this amount of time before it can fire. It is possible that the transition becomes disabled while waiting to fire. For example, in Figure 10, t0 can be disabled while waiting (regardless of decision rule) if t1 becomes enabled and fires. Note that in the figure a double bar represents a transition whose processing time is non-zero. A single bar represents a transition with zero processing time; it fires as soon as it is enabled.

Place-timed SPN. In place-timed SPN's, the processing times are associated with places. When a token enters a place, it initially becomes "unavailable" to the rest of the system until the corresponding probabilistically chosen processing time elapses. A transition is not enabled unless all its input arcs are

[9]No SPN developed so far has attempted to assign transition times to both transitions and places.

connected to places with "available" tokens. Figure 11 shows an example of place-timed SPN's. A double circle in the figure represents a place with non-zero processing time, while a single circle represents a place with zero processing time.

A place-timed SPN can be converted to a transition-timed SPN that has the same dynamic property; however, the converse of this statement is not true in general. For example, the transition-timed SPN fragment depicted in Figure 10 has no equivelence in the place-timed format[10]. Nevertheless, in many modeling problems place-timed SPN's offer more concise structure than transition-timed SPN's (Fig. 12), making model interpretation easier. This is especially true in modeling of the cardiac electrical conduction system, and the issue of choosing one of the two SPN formats is addressed breifly in the next subsection. Both formats can be seen regularly in the literature, although transition-timed SPN's seem to be a little more popular.

3.3 SPN for Modeling of Cardiac Conduction System

SPN modeling of the cardiac electrical conduction system poses a tradeoff between using the place-timed and transition-timed versions: *(i)*Place-timed SPN's offer a graphically more concise format to represent the cardiac system than transition-timed SPN's. For example, compare the normal heart models using the two SPN formats(Fig. 2c and 2d). *(ii)*Transition-timed SPN's can model a wider range of dynamics than place-timed SPN's. Unfortunately, some dynamic aspects of the cardiac system can only be modeled with the transition-timed format. An example of such is activation of a tissue during its relative refractory period. The SPN model of relative refractory period (Fig. 14d-1) is almost identical to the transition-timed SPN of Figure 10, which cannot be translated into a place-timed SPN. We emphasize that the graphical conciseness offered by place-timed SPN's is important, as we will see in the

[10]This statement holds if the "race firing policy"[7] is adopted. In the literature this policy is seldom seen, and statements asserting equivalence between place- and transition-timed formats can be found. There is, however, no single SPN format preferred over the others today, and such statements are not well founded.

next section that some relatively simple models of cardiac arrhythmia can have complex topologies. Graphical conciseness facilitates not only interpretation of the models but also representation of more complex physiological mechanisms. On the other hand, the transition-timed format is necessary to represent certain essential dynamical properties of the cardiac system. This dilemma can be avoided in the following way: As we have mentioned, every place-timed SPN has an equivalent transition-timed SPN. We can thus graphically represent a system with a place-timed SPN but deal with its dynamics in terms of its transition-timed equivalence. This relation between place-timed SPN's and transition-timed SPN's is analogous to that between high level computer languages and assembly codes as compliers translate the high level languages into assembly codes before executable codes are generated.

To represent a model with a place-timed SPN while dealing with its dynamics with the corresponding transition-timed SPN, we need to allow the place-time format to represent just as wide range of dynamics as the transition-timed format. We, thus, make a modification in the place-timed SPN format by introducing "interruptable processing times." A place with an interruptable processing time has a special output arc through which a token inside it is always "available" to the rest of the system. Figure 13a shows such a place. It has a special output arc, marked by a small circle, through which the token inside it is always available to the rest of the system. Thus, while the transition t0 cannot fire until the processing time at the place elapses, t1 can fire as soon as it is enabled. Firing of t1, therefore, may "interrupt" the processing time assigned to the place. As previously mentioned, a standard place-timed format cannot replace the transition-timed SPN fragment of Figure 10, but with an interruptable processing time that is possible(Fig. 13c). This illustrates the usefulness of the new place-timed SPN's. Although this modified place-timed format (i.e., using interruptable processing times) is not found in the literature, its execution is exactly the same as the standard transition-timed format under the "race" firing policy. For example, the modified place-timed SPN of Figure 13a behaves exactly the same as the transition-timed SPN of

Figure 13b. That is, a modified place-timed SPN can always be converted into a standard transition-timed SPN, whose execution policy is well-defined. We will be using this modified place-timed SPN format in the next section.

4 SPN Models of Cardiac Arrhythmias

In Section 2 we modeled several common cardiac arrhythmias with networks of rhythm and transmission elements. In this section we implement various rhythm and transmission elements with SPN's. We then discuss briefly how to connect these SPN elements to form SPN cardiac arrhythmia models. Finally, we present several examples of such SPN models of cardiac arrhythmias at the end of the section. The graphical notations in the figures of this section are the same as the previous sections. In particular, the modified place-timed SPN's are denoted as in Figure 13: double circles represent places with non-zero processing times, and output arcs marked by small circles are the "interruptable" outlets of tokens from such places.

4.1 Fundamental Building Blocks

Recall form Section 2 that variations in autorhythmic rates, conduction delays, and refractory periods characterize functions of individual rhythm and transmission elements which are in turn responsible for most cardiac arrhythmias. We now present SPN implementations of sub-elements ("units") controlling these timing quantities.

1)Autorhythmic unit.

Figure 14a shows the basic SPN building block for an autorhythmic unit. The period of the rhythm is represented by the processing time associated with the single place p0. The transition t1 represents the output of the autorhythmic unit. The incomplete arcs to and from t1 are parts of the SPN fragment representing the neighboring tissue which receives excitation from the autorhythmic unit. The reception of excitation is accomplished by firing of t1. As soon as the token becomes availabe in p0, it is fired back into p0 via either t0 or t1 to recycle the process. An autorhythmic activity may or may not induce activity in the neighboring tissue depending on whether the tissue is in refractory period or not. But if the tissue is ready to be excited, the activity is always transferred to it. Thus, the decision rule for the conflict set $\{t0, t1\}$ is assigned

so that it chooses t1 preferentially over t0.

2)Conduction units.

A conduction unit receives excitation from one tissue (the input tissue), waits for a probabilistically specified amount of time (the conduction delay), and transfers the excitation to another tissue (the output tissue). Figure 14b shows the SPN implementation of the basic conduction unit. If the token in the place p1 is "available" (meaning that the conduction tissue has come out of the refractory period and is excitable), the transition t0 fires when it receives excitation from the input tissue. The token then enters the place p0 whose processing time represents the conduction delay. After the delay, the token is fired back into p1 by t1 or t2. When the token is in p0, t1 is always enabled while t2 is enabled only when the output tissue is ready to receive the excitation. Since excitation is always transferred to output tissue not in its refractory period, the decision rule is assigned so that t2 is preferentially chosen over t1 whenever they are in conflict. The processing time associated with p1 represents the time required for the conduction unit to become ready to receive a new excitation after it has processed a preceding excitation; thus, this processing time can be considered as a collective absolute refractory period for all the cells in the conduction tissue. The roles of relative refractory periods in conduction of excitations is discussed later.

3)Refractory periods.

There are two kinds of refractory periods–absolute and relative. When the tissue is in an absolute refractory period, an oncoming excitation is blocked. On the other hand, when the tissue is in a relative refractory period, an oncoming excitation induces the tissue to be activated with abnormal characteristics such as elongated conduction delay (e.g., Wenckebach). Figure 14c shows a basic absolute refractory unit. The processing time assigned to the single place is the absolute refractory period, and the transition cannot fire unless the token in the place becomes available. Figure 14d-2 shows a basic relative refractory unit, using a place with an interruptable processing time introduced in Section 3. The processing time associated with the place represents the rela-

tive refractory period. The firing of t0 represents the normal course of action where the tissue becomes completely ready to receive a new excitation. On the other hand, the firing of t1 represents a premature activation of the tissue by an external excitation (an interrupt), and the tissue is expected to display some abnormal activities. Figure 14d-1 shows the transition-timed equivalent of the relative refractory unit. As mentioned in the previous section, these two SPN's display exactly the same dynamics.

4.2 SPN Model of the Normal Heart

Using the building blocks developed above, a SPN model of the normal heart can be implemented. We have shown in Section 2 that the normal heart can be modeled with three elements — the SA node, AV node, and ventricles(Fig. 2b), and these elements can respectively implemented as the autorhythmic unit, conduction unit, and absolute refractory unit described above. The resulting SPN model is shown in Figure 2c. The output of the model is the timing of generation of P and R waves, and these are represented by firing of the transitions t0, t1, and t3 — t0 and t1 for P wave and t3 for R wave. The parameters of the model are the processing times associated with the places p0, p1, p2, and p3, and these correspond with the autorhythmic interval of the SA node, the refractory period of the AV node, conduction delay of the AV node, and the refractory period of the ventricles, respectively. The transition-timed equivalent is shown in Figure 2d, and note that the model in this format requires twice as many nodes as the model in the place-timed format. Figure 2e shows the output of a simulation run of the SPN model in Figure 2c. (As mentioned before, short and long vertical lines represent P waves and R waves, respectively, and tick marks have one second intervals.) The processing times used in the simulation run are listed on Table 1.

The simplicity of the models in Figure 2 has come about because unnecessary physiological details are deliberately left out. For example, in the signal flow block diagram model (Fig. 2b), uni-directional transmission element rather than more complex bi-directional transmission element was used

to represent the AV node because it is known that no retrograde conduction is observed in a normal P,R wave sequence. The rhythm element representing the SA node does not need an input terminal also because of the absence of retrograde conduction. We emphasize that the normal heart is still capable of conducting excitations in the retrograde direction, but modeling at such level of physiological accuracy is not necessary to capture the behavior of a normal P,R wave sequence correctly. Using such simpler variations of the rhythm and transmission elements allows simpler SPN implementations of them. In this case we were able to directly substitute the autorhythmic unit from Subsection 4.1 for the rhythm element representing the SA node, the conduction unit for the transmission element of the AV node, and the absolute refractory unit for the rhythm element of the ventricles. We have seen in Section 2, however, that more complex variations of these elements are needed to model most cardiac arrhythmias. In the next subsection we extend the basic SPN units of the previous subsection to implement a wider variety of rhythm and transmission elements.

4.3 Rhythm and Transmission Elements

The rhythm and transmission elements are aggregations of the fundamental building blocks developed above. SPN implementations of various rhythm and transmission elements are presented.

Rhythm Elements.

The most simple rhythm elements are the pacemaker (Fig. 15a) and terminal (Fig. 15f). An example of a pacemaker is the SA node in the normal heart; the sole function of the element is to generate excitation periodically. The single parameter for the pacemaker is the period of the autorhythmic excitation, and this is represented by the processing time at the place. An example of a terminal is the ventricle in the normal heart; the element simply receives and absorbs incoming excitations. The single parameter of the terminal is the absolute refractory period. If the terminal depicted on Figure 15f represents the ventricle, firing of the transition represents the generation of the R wave.

In reality, pacemaker tissues can receive excitation (for example, the SA node can receive retrograde-conducting excitation) and can be reset or stunned. A more accurate model of pacemakers should have such dynamic properties. Moreover, a way to make the model more accurate than this is to include an absolute refractory period during which the pacemaker tissue cannot be reset or stunned. These functional variations of the rhythm element can be used in arrhythmia modeling, and corresponding SPN building blocks are presented in Figure 15:

- the basic pacemaker (Fig. 15a)
- resettable pacemaker (Fig. 15b)
- stunnable pacemaker (Fig. 15c)
- resettable pacemaker with refractory period (Fig. 15d)
- stunnable pacemaker with refractory period (Fig. 15e)
- the basic terminal (Fig. 15f)

Transmission Elements.

The most simple transmission element is the basic uni-directional transmission element depicted in Figure 16a and employed in the construction of the normal heart model (Fig. 2b). One of the functional variations is the transmission element with a probability of conduction, shown in Figure 16b, which is necessary in the modeling of second degree AV block. An extra transition t0 has been added. The transitions t0 and t1 are in conflict; firing of t0 does not activate the transmission element while firing of t1 does. The decision rule for the conflict set {t0, t1} is a probabilistic policy where the probability "q" of choosing t1 is equal to the probability of the conduction.

Another functional variation is the bi-directional transmission element. It is more realistic than the uni-directional element, while its implementation is slightly more complex than a simple combination of two uni-directional elements. The complexity is due to the necessity of modeling annihilation of two excitations colliding inside the element. Figure 16c shows the bi-directional transmission element. It is basically two uni-directional elements superim-

posed, with the addition of the transition t5 and the use of interruptable processing times at p0 and p1. When excitations collide in the element, t5 fires, and no activity reaches the outputs.

Another functional variation is the transmission elements capable of generating the Wenckebach phenomenon. As discussed in Section 2 the Wenckebach phenomenon is charcterized by an incrementally increasing P,R sequence. An abnormally long refractory period at the AV node is thought to be responsible for the phenomenon. Specifically, after the AV node is excited by a normal excitation from the SA node, the relative refractory period of the node is just long enough such that the next normal excitation arrives at the AV node during a late part of the relative refractory period. The AV node still becomes excited, but the subsequent conduction delay as well as absolute and relative refractory periods are longer than previous ones. Consequently, the next normal excitation tends to arrive at the AV node during an even earlier part of the relative refractory period, resulting in yet longer conduction delays and refractory periods. Such an incremental increase in the AV node conduction delay (and thus the P,R wave interval) continues until the normal excitation arrives at the node during an absolute refractory period, resulting in a blocked conduction (and thus a missing R wave). When a conduction block occurs, the AV node gains enough time to recover from its refractory period completely; then, the process described above begins again.

Figure 16d shows an SPN implementation of a transmission element that captures such cyclic process. The relative refractory period is represented by the interruptable processing time of p0. The normal course of token movement is p0 – p1 – p2 – p3 – p0. However, when the element is excited during its relative refractory period, the token travels the abnormal course p0 – p4 – p5 – p0. The conduction delays through the element are represented by p2 and p4, while the absolute refractory periods are represented by p3 and p5. For the Wenckebach phenomenon, the processing times for p4 should be set longer than for p2 while that for p3 should be longer than for p5. We have mentioned in Section 2 that this element should have "memory." The element

in this example registers whether the previous excitation has arrived during its relative refractory period or not by the location of the token, i.e., whether the token is in the abnormal loop or the normal loop. Note that the token takes a longer time to go through the abnormal loop so that the chance of receiving the next external excitation while it is in absolute or relative refractory period is greater. To model common Wenckebach conditions, more than one abnormal loop may be necessary. Such a Wenckebach model is presented in Subsection 4.5.

Several functional variations of the transmission element have been discussed here. Although their coverage is not exhaustive, most of common cardiac arrhythmias can be modeled using the variations of the elements discussed above. The SPN implementations of these are presented in Figure 16:

- the basic uni-directional transmission element (Fig. 16a)
- uni-directional transmission element with probability of block (Fig. 16b)
- bi-directional transmission element (Fig. 16c)
- a stunnable transmission element (Fig. 16d)

4.4 Interfacing the Elements

Here, we discuss ways to connect the SPN representations of rhythm and transmission elements described above.

Case I: connecting a single output to multiple inputs. Figure 17a shows a rhythm element sending excitation to two transmission elements. When the rhythm element sends an excitation, each of the two receivers (the transmission elements) can be in two states— ready to receive the excitation or not ready to receive. Thus, the number of states of the receivers is four ($= 2^2$), and four transitions are used to implement this interface with SPN (Fig. 17b). Each of the four transitions represent the following cases:

t0 – neither of the transmission element is ready to receive.

t1 – element A is ready to receive, but not element B.

t2 – both elements are ready to receive.

t3 – element B is ready to receive, but not element A.

In general, when a single output is trying to distribute an excitation to N inputs, 2^N transitions are required.

Case II: connecting multiple outputs to a single input. Figure 18a shows three rhythm elements sending excitation to a transmission element. Since each sender may or may not be able to excite the receiver, six ($= 2 \times 3$) transitions are needed (Fig. 18b). In general, when N outputs are trying to access to a single input, $2N$ transitions are required.

4.5 SPN Models of Cardiac Arrhythmias

SPN implementations of the cardiac arrhythmias discussed in Section 2 are presented in Figures 3c to 8c. The results of simulation based on these SPN's are presented in Figures 3b to 8b, in which the normal P waves are represented by short lines and normal R waves by long lines. The values of the model parameters used in the simulation runs are listed in Table 1.

Atrial Premature Beat (Fig. 3c)

The block diagram model of Figure 3a is implemented with an SPN. Two "resettable pacemakers" are used to represent the normal (SA nodal) and ectopic rhythm sources in the atria. Firing of one source resets the other source; thus, after every beat the two sources race to initiate the next excitation. The processing times at p0 and p1 correspond with the autorhythmic intervals of the ectopic and normal sources, respectively. The probability density function of the processing time at p0 has a broader distribution than the one at p1, so that with a certain probability the ectopic source can generate excitation at a noticablly shorter interval than the normal source. The firing of t0 or t1 represents an excitation of the ectopic source, and it produces a P wave with an abnormal morphology, denoted by a "P" with an overbar in the figure. The firing of t2 or t3 represents an SA nodal excitation producing a normal P wave. The rest of the model is similar to the normal heart model. The places p3 and p2 represent the AV nodal conduction delay and its refractory period, respectively, and they are parts of the "basic uni-directional transmission el-

ement." The ventricles are modeled by the "terminal" element (p4 and t5). Firing of t5 produces a R wave. In the simulation result (Fig. 3b), the short vertical lines with small squares at their tips represent P waves initiated by the ectopic source (i.e., the premature beats).

Ventricular Premature Beat (Fig. 4c)

This model, whose block diagram was introduced in Fig. 4a, consists of two "resettable pacemakers with refractory periods" and a single "bi-directional transmission element." The places p1 and p0 are the autorhythmic interval and absolute refractory period at the SA node, respectively, while p7 and p6, respectively, are those at the ventricles. The conduction delay and absolute refractory period at the AV node are represented by p3 and p4, respectively, for the antegrade (normal) direction and by p2 and p5, respectively, for the retrograde direction. Correspondence between firing of the transitions and production of the waves are as follows: t2 and t3 for normal P, t5 for normal R, t6 and t7 for ectopic (premature) R, and t1 for retrograde P. In the simulation result(Fig. 4b), the R waves and P waves with small square on the tips denote the ectopic R waves and retrograde P waves, respectively. Observe that a pairing of a normal P wave and an ectopic R wave occuring at about the same time is followed by neither a normal R wave nor a retrograde P wave. Nearly simultaneous autorhythmic excitations at the two rhythm sources of the model produce a normal P and ectopic R waves, but the resulting flows of excitations have collided inside the transmission element and blocked each other.

Bigeminy (Fig. 5c)

As described in Section 2, we use the concept of "reentrant pathway" to explain the mechanism of bigeminy. The model is almost the same as the normal heart model. The only difference is the presence of the reentrant pathway represented by the basic uni-directional transmission element consisting of p3 and p5. When the excitation is passed from the AV node to the ventricles (which is modeled by the "terminal" element consisting of p4) via the transition t4, the reentrant pathway is excited. The reentrant pathway delays the excitation by an amount specified by the processing time at p3 and then passes it to the

ventricles via t5. Firing of t5 produces abnormal R waves which are denoted by long lines with small squares in the simulation result(Fig. 5b). The time intervals between a normal R wave and the succeeding abnormal R wave are fairly constant, exhibiting a coupling interval. Note that a normal P wave follows every abnormal R wave. In reality such a P wave cannot be easily discerned in an ECG tracing because of the typical, broad shape of the abnormal R waves of bigeminy.

Second Degree AV Block (Fig. 6c)

The topology of this model is exactly the same as that of the normal heart, but in this model "uni-directional trasmission element with probability of conduction" is used to represent the AV node. Thus, the decision rule for the conflict set {t0, t1} is no longer determinstic (i.e., to preferentially choose t1 over t0). Whenever a conflict exists, t1 is chosen over t0 with a probability equal to the probability of conduction. Figure 6b is the result of simulation of a "4:3 Block," where the probability of conduction is $\frac{3}{4}$. Since in this model conduction blocks are independent events, they can occur in consecutive beats. In reality, however, such consecutive blocks are rare. Making sure that conduction blocks are isolated can be accomplished at the expense of a more complex model with more memory. Specifically, decision by the model to cause a block in a particular beat must be influenced by whether or not a block has occurred in the previous beat, i.e., the model must have a "memory" of an event in the previous beat. Although such a model is not presented in this paper, the model of the Wenckebach phenomenon described next contains a memory feature of the same general type as that would be needed to obtain a more accurate model of second degree AV block.

Wenckebach (Fig. 7c)

The block diagram of this Wenckebach model consists of two rhythm elements and a transmission element(Fig. 7a). Two "basic rhythm elements" are used to represent the SA node (p0) and ventricles (p12). The single transmission element is a "stunnable transmission element" similar to the one described in Subsection 4.3 and Figure 16d, but this element has two extra abnormal

loops." The loops, in the order of increasing transit times, are: (i)p1 – p2 – p3 – p4 – p8, which is the normal loop, (ii)p1 – p2 – p3 – p5 – p9, (iii)p1 – p2 – p6 – p10, and (iv)p1 – p7 – p11. The processing times at p4, p5, p6, and p7 (in the order of increasing length) represent the AV conduction delays (thus the P,R intervals). Those at p8, p9, p10, and p11 are the absolute refractory periods of the AV node. The relative refractory period is divided into three sub-periods of equal lengths — early (p1), middle (p2), and late(p3). Each of these sub-periods is assigned an interruptable processing time. An interrupt occurs when the SA node (p0) excites while the token of the AV node is in one of these relative refractory sub-periods, initiating an entry into the corresponding abnormal loop. P waves are produced by the firing of t0, t1, t2, t3, or t4, while R waves by the firing of t8, t10, t12, or t14. The simulation result(Fig. 7b) clearly displays the Wenckebach phenomenon.

Wolfe-Parkinson-White Syndrome (Fig. 8c)

This model uses "basic" elements for the SA node (p0–autorhythmic interval) and AV node (p3–conduction delay, p2–refractory period). The ventricles are divided into two parts: one part receives excitation from the bundle of Kent and produces delta waves, while the other part receives excitation normally and produces normal R waves. Both of these are modeled with the "terminal" rhythm elements (p5 and p6). The bundle of Kent is represented by the uni-directional transmission element consisting of p4 (conduction delay) and p1 (refractory period). Delta waves and normal R waves are produced when t6 and t5 fire, respectively. P waves are produced when t0, t1, t2, or t3 fires. In the simulation result(Fig. 8b) the delta waves are represented by short lines with squares at the tips, and they are immediatedly followed by R waves as they should. Note that in the model the two parts of the ventricles (p5 and p6) could have been connected with a bi-directional transmission elements since physiologically they are parts of a single block of tissue. It is clear from the simulation result, however, that these two parts are excited almost simultaneously so that collision of excitations in such a transmission element is evident. Thus, to achieve the most concise modeling of the P,R sequence

such an element is not included.

This section along with Section 2 has illustrated a systematic way in which we can derive SPN's for cardiac arrhythmia models. Specifically, the physiological mechanism of an arrhythmia is first described as a signal flow block diagram with rhythm and transmission elements. The block diagram may be simplified greatly by removing physiological details unnecessary to characterize the P,R sequence of the particular arrhythmia under study. Such a high level description can then be translated into an SPN in an element-by-element fashion using the implementations presented in this section (and straightforward extensions of them if needed). Thus, we have a method to derive the SPN structure (topology), initial token placement, and decision rules. The last piece of information required to complete the model are the parameters, i.e., probability distributions for the processing times and probabilistic descision rules. We emphasize that two sets of parameters assigned to the same SPN structure can lead to two outputs drastically different from each other. For example, the SPN structure for Bigeminy (Fig. 5c) can be programmed to output a P,R sequence of Trigeminy, a different arrhythmia class[11], just by increasing the processing time at the place p3 by one second.

Given a P,R sequence to be modeled, some parameters such as the SA nodal rhythms and AV conduction delays have direct correspondence to the given data and are thus relatively easy to assign; however, many other parameters such as refractory periods cannot be directly observed from the data and must be chosen intelligently. The parameter values listed in Table 1 are chosen so that the simulation results match with the qualitative characteristics of a P,R wave sequence for a given cardiac arrhythmia as described in Section 2, under the constraint that each value chosen must be physiologically plausible.

[11] An abnormal R wave appears every three cycles in Trigeminy in contrast to every two cycles in Bigeminy.

5 Conclusion

5.1 Summary

This thesis has described a systematic procedure for constructing concise mathematical models capable of generating the P,R wave patterns characteristic of different arrhythmias. In particular, there is a straightforward way in which one proceeds from a phenomenological descriptions to a block diagram and then to a stochastic Petri net. Fundamental to this modeling methodology is the availability of electrophysiological explanations for the phenomena characterizing various cardiac arrhythmias. The modeling methodology, in turn, offers a general, abstract framework to synthesize and analyze physiological hypotheses pertaining to electrical activities in the heart.

A key feature of the models presented here is the hierachical separation of model structures and parameters. The model structure captures the particular aspects of cardiac physiology of importance in modeling an arrhythmia. Specifically, the model structure is determined by the interactions among the rhythm and transmission elements and dynamics of each of these elements. The model structure characterizes the distinct features of various arrhythmias at different levels of physiological detail. For example, while the normal heart and atrial premature beat are distinguishable at the level of the signal flow block diagram (i.e., compare Figures 2b and 3a), the normal heart and Wenckebach are not (Fig.'s 2b and 7a). The later pair can only be distinguished by the inner dynamics of the transmission element at the AV node; the corresponding Petri net structures (Fig.'s 2d and 7c) which reflect these dynamics are indeed distinct from each other.

The parameters of the models, on the other hand, provide us with the means for modeling the synchronization and control among the cardiac elements and for including the expected level of statistical fluctuation in the observed wave sequence. Although the parameters play a role in arrhythmia characterization at a finer level than the model structures, they are indispensible in complete characterization and are often pivotal in distinguishing some

arrhythmic phenomena. For example, as mentioned previously, the stochastic Petri net in Figure 5 can produce wave sequences corresponding with both Bigeminy and Trigeminy depending on the value of the conduction delay parameter for the reentrant pathway. Similarly, if the SA rate were sufficiently slow in the Wenckebach model, the Wenckebach phenomenon would not be observable, as the AV node would have sufficient time to recover from refractory periods between successive excitations.

The modeling methodology presented in this work is expected to be applicable to a wide range of electrical phenomena in the heart because of its physiological basis. It is also flexible in the sense that modeling at various complexity levels is possible. From the perspective of designing an arrhythmia classification algorithm, being able to control the model complexity, in response to the numbers and types of different classes considered, is an obvious advantage.

5.2 Possible Extensions

Selection of model parameters

An important area for further work is development of algorithms that estimate the values of the model parameters to realize a desired P,R sequence. Since the parameters tend to represent physiological quantities (e.g., SA rate), the estimates should be within physiologically reasonable ranges of values. Parameter estimation is not only an integral part of model construction but also likely to be the first stage of an arrhythmia classification algorithm. Note that some parameters, such as refractory periods in most cases, are not directly measureable from the wave sequence data. Consequently, in posing the parameter estimation problem one must include some analysis of how each SPN parameter affects the model output.

Design of classification algorithm

As mentioned before, a potential approach in classification is computation of likelihoods by an iterative procedure. In particular, Doershuck[2] has presented an iterative, distributed algorithm for computation of state trajectories in the "interacting Markov chain" models, and the computation of the likelihoods involve the evaluation of such estimated trajectories. An important aspect of this approach is aggregation of parts of the model in order to facilitate computation. That is, some selected portions of the model are drastically simplified by statistical approximations during certain iterative steps of state trajectory estimation. Applying a similar computational procedure to SPN models is expected to be a promising alternative because of their natural hierachical model structure which provide a natural basis for aggregation. Also, in the Petri net literature, work directed towards statistical characterization of various dynamic properties of SPN's are available (e.g. [9] and [14]); these might be useful in approximating, in a statistically aggregated manner, the dynamics of various parts of the model.

Generalization of modeling methodology

Another possible direction of research is to extend the "physiological modeling" concept to describe a wider variety of electrical activities in the heart. A potentially useful extension is to partition the cardiac conduction system at a finer level. For example, in this work the ventricles have been considered as a single entity within the cardiac conduction system. Although such a treatment of the ventricles has been sufficient for the purpose of describing the P,R wave sequences of arrhythmias, a wider range of ECG phenomena may be characterized with SPN models by partitioning the ventricles in some way and dealing with each of the elements of such a partition as though it is capable of independent rhythmic and conductive activities.

References

[1] Bonner, R. E. and Schwetman, H. D. "Computer diagnosis of electrocardiograms. III. A computer program for arrhythmia diagnosis." *Comput. and Biomed. Research*, vol. 1, pp. 387–407, 1968.

[2] Doerschuk, P. C. "A Markov chain approach to electrocardiogram modeling and analysis." Ph. D. Thesis, Massachusetts Institute of Technology, 1985.

[3] Gersch, W. *et al.* "Cardiac arrhythmia classification: A heart-beat interval–Markov chain approach." *Comput. and Biomed. Research*, vol. 3, pp. 385–392, 1970.

[4] Gustafson, D. E. *et al.* "ECG/VCG rhythm diagnosis using statistical signal analysis, Part I and II." *IEEE Trans. Biomed. Eng.*, vol. BME-25(4), pp. 344–361, 1978.

[5] LeBlanc, A. R. and Roberge, F. A. "Present state of arrhythmia analysis by computer." *Can. Med. Assoc. Jour.*, vol. 108, p.1239, 1973.

[6] Marriott, H. J. L. *Practical Electrocardiology*, Williams and Wilkins, Baltimore, 1977.

[7] Marsan, M. A. *et al.* "On Petri nets with stochastic timing." in *International Workshop on Timed Petri-Nets 1985*, pp. 80–87.

[8] Milnor, W. R. "Properties of cardiac tissues." in V. B. Mountcastle ed., *Medical Physiology*, 14th ed., Ch. 36, Mosby, St. Louis, 1980.

[9] Molloy, M. K. "Performance analysis using stochastic Petri nets." *IEEE Trans. Comput.*, vol. C-31(9), pp. 913–917, 1982.

[10] Peterson, J. L. "Petri nets." *Computing Surveys*, vol. 9(3), pp. 223–252, 1977.

[11] Peterson, J. L. *Petri Net Theory and the Modeling of Systems*, Prentice-Hall, Englewood Cliffs, NJ, 1981.

[12] Ramamoorthy, C. V. and Ho, G. S. "Performance evaluation of asynchronous concurrent systems using petri nets." *IEEE Trans. Software Engineering*, v.SE-6(5), pp. 440–449, 1980.

[13] Wallace, A. G. "Electrical activity of the heart." in J. W. Hurst ed., *The Heart*, 6th ed., Ch. 4, McGraw-Hill, New York, 1986.

[14] Wiley, R. P. "Performance analysis of stochastic timed petri nets." Ph. D. Thesis, Massachusetts Institute of Technology, 1986.

[15] Willems, J. L. and Pipberger, H. V. "Arrhythmia detection by digital computer." *Comput. and Biomed. Research*, vol. 5, pp. 263–278, 1972.

Figure and Table Captions

Figure 1

Building blocks for the signal flow models: a rhythm element(a) and transmission element(b).

Figure 2

Models of normal heart P,R sequences: (a)–a physiologically motivated signal flow model, (b)–a simplified signal flow model, (c)–SPN implementation of (b) using the place-timed format, and (d)–SPN implementation using the transition-timed format. A P,R sequence output of model (c) is shown in (e).

Figure 3

Atrial premature beat: signal flow model(a) and an example of P,R sequence(b) obtained by the simulation of the SPN implementation(c) of the model.

Figure 4

Ventricular premature beat: signal flow model(a) and an example of P,R sequence(b) obtained by the simulation of the SPN implementation(c) of the model.

Figure 5

Bigeminy: signal flow model(a) and an example of P,R sequence(b) obtained by the simulation of the SPN implementation(c) of the model.

Figure 6

Second degree AV block: signal flow model(a) and an example of P,R sequence(b) obtained by the simulation of the SPN implementation(c) of the

model.

Figure 7
Wenckebach phenomenon: signal flow model(a) and an example of P,R sequence(b) obtained by the simulation of the SPN implementation(c) of the model.

Figure 8
Wolfe-Parkinson-White syndrome: signal flow model(a) and an example of P,R sequence(b) obtained by the simulation of the SPN implementation(c) of the model.

Figure 9
An example of Petri net.

Figure 10
A portion of a transition-timed SPN.

Figure 11
An example of place-timed SPN.

Figure 12
Equivalence of two SPN formats: the place-timed SPN fragment in (a) can be translated into the transition-timed format as shown in (b), using additional nodes.

Figure 13
A modified place-timed format that includes interruptable processing time:

the SPN fragment in the modified place-timed format shown in (a) is dynamically equivalent with that in the transition-timed format shown in (b). Also, the SPN fragment in (c) (modified place-timed) is dynamically equivalent with that in Figure 10 (transition-timed), which cannot be translated into the standard place-timed format under the "race" execution policy defined in the reference [6].

Figure 14
Fundamental units for SPN implementation of signal flow models.

Figure 15
SPN implementations of common rhythm elements. The processing time assigned to a places is period of autorhythmicity (denoted as "rhythm" in the figure), absolute refractory period ("refra"), or duration of stunning ("stun").

Figure 16
SPN implementation of common transmission elements: (a)–basic uni-directional, (b)–uni-directional with probability of conduction "q", (c)–bi-directional, (d)–uni-directional and stunnable.

Figure 17
An example of interfacing SPN blocks — fan-out: (a)–The rhythm element sends its output to two transmission elements. (b)–The SPN implementation of interface of the three elements in (a).

Figure 18
An example of interfacing SPN blocks — fan-in: (a)–Each of the three rhythm elements can activate the transmission element. (b) The SPN implementation of interface of the four elements in (a).

Table 1

Model parameters: The processing times and probabilistic decision rules for the models in Figures 2 to 8 are shown. The processing times take the discrete values listed here. They are uniformly distributed among the indicated set of values unless noted otherwise. The unit of time is the *second*.

Figure 1

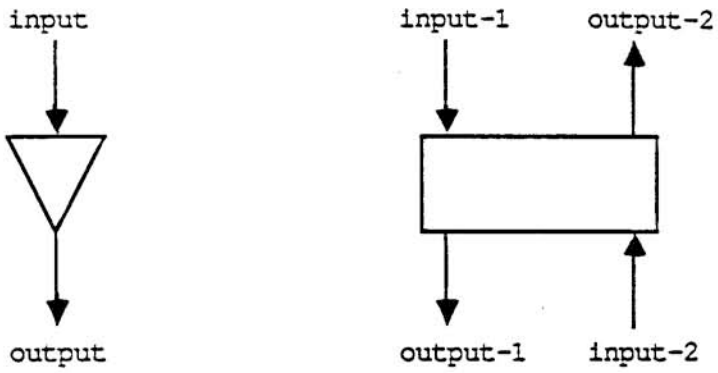

(a) (b)

Figure 2

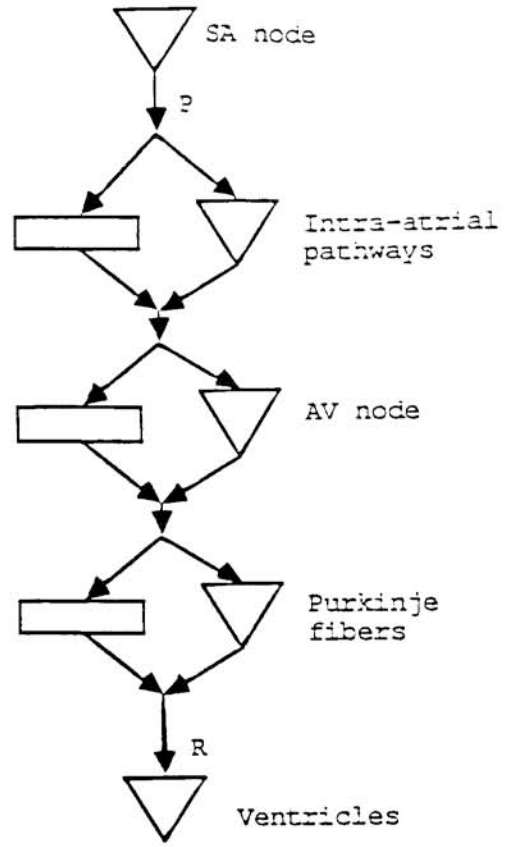

(a)

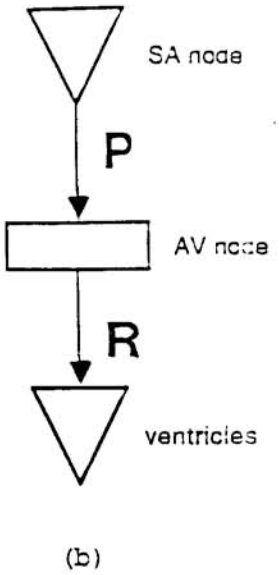

(b)

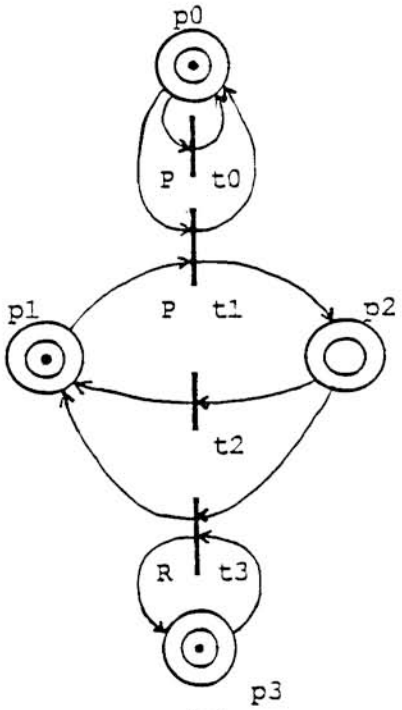

(c)

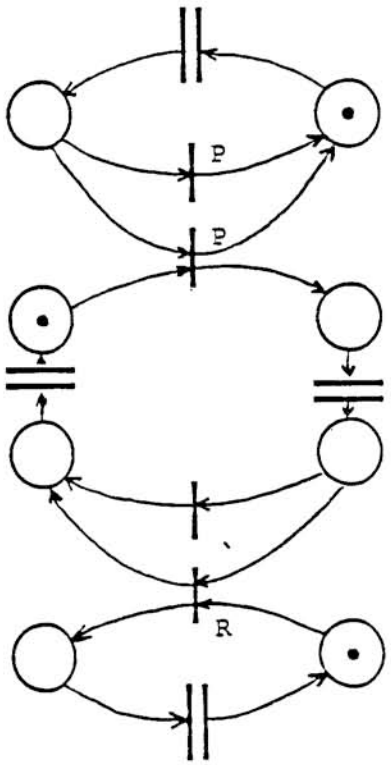

(d)

(e) Normal heart P,R sequence

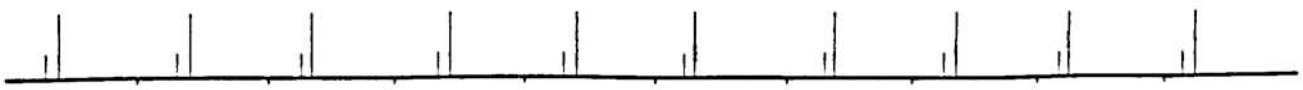

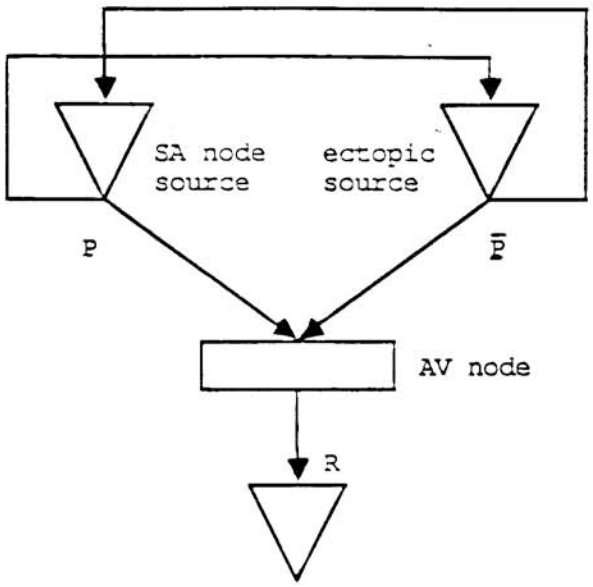

(a)

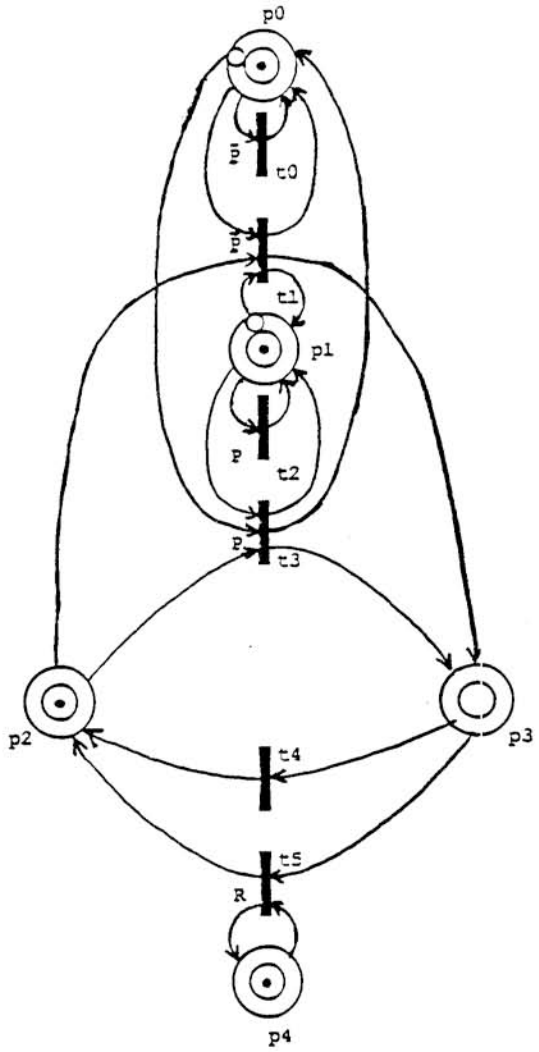

(c)

Atrial Premature Beat

(b)

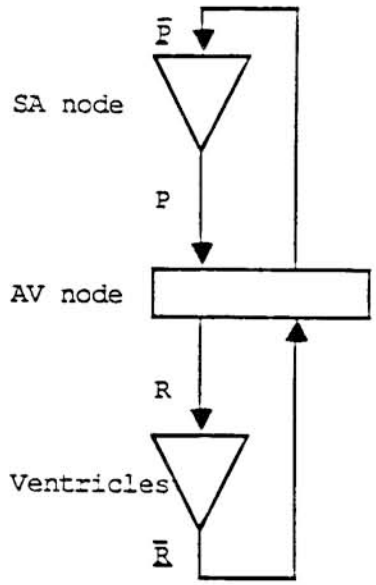

(a)

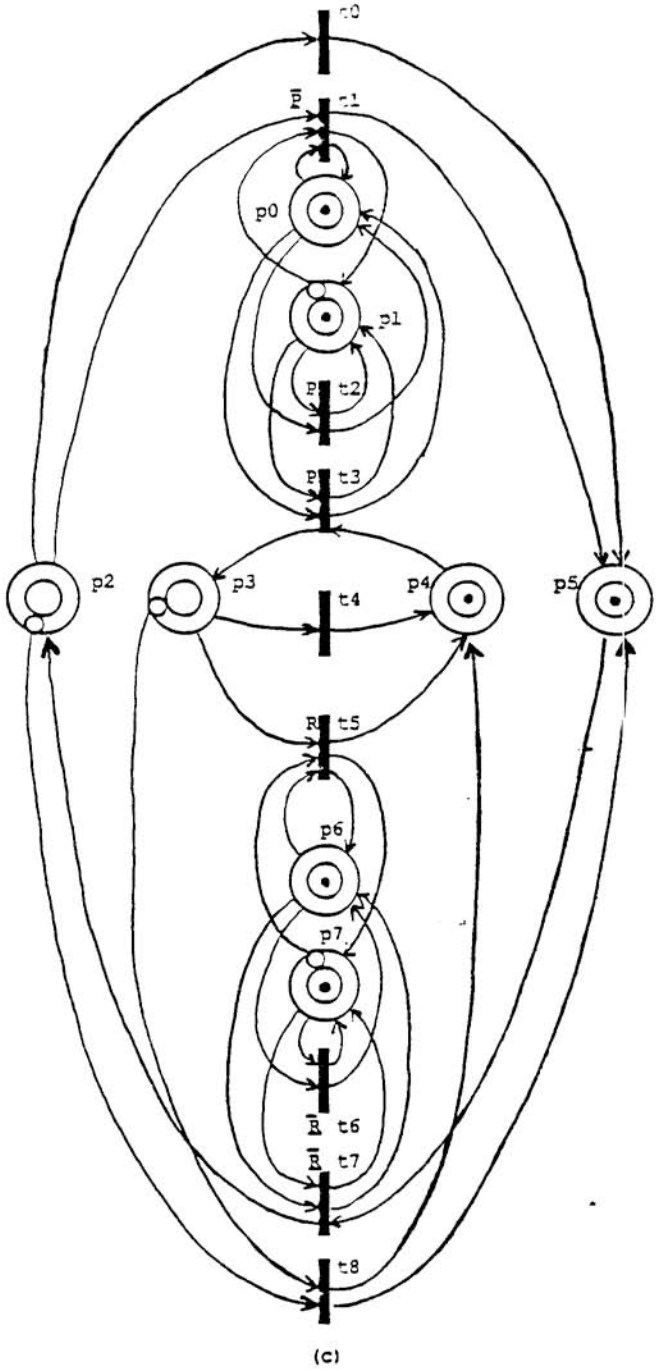

(c)

Ventricular Premature Beat with retrograde P wave

(b)

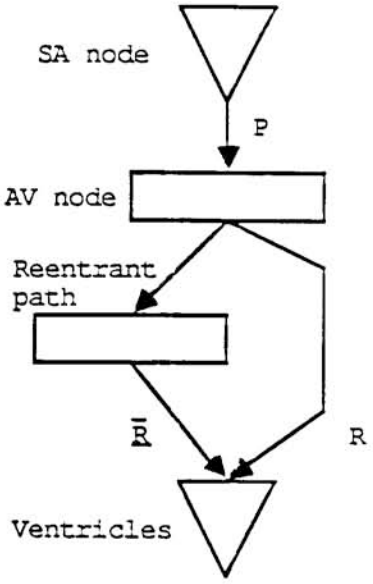

(a)

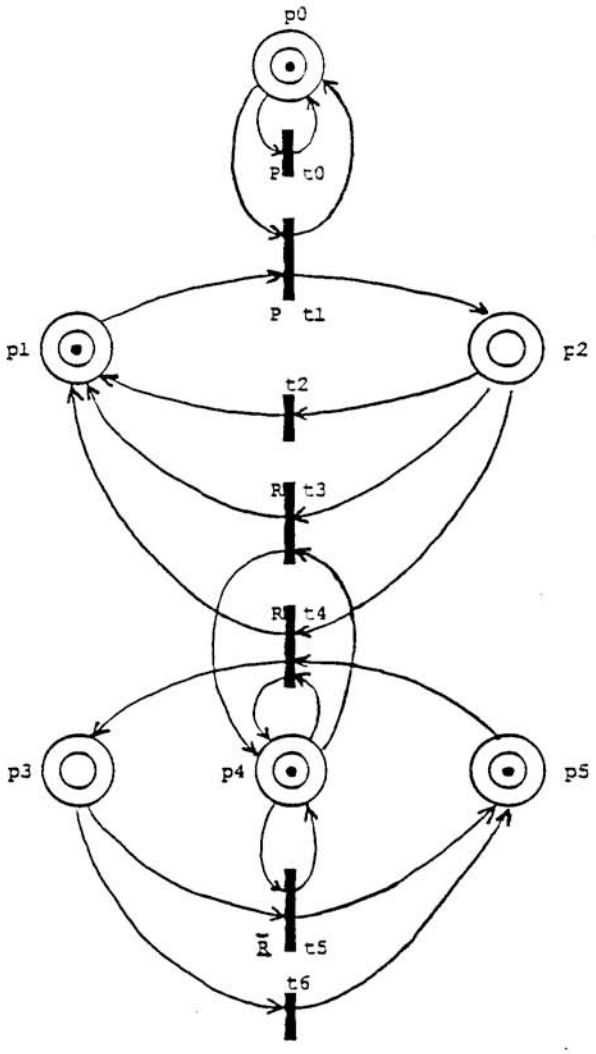

(c)

Bigeminy

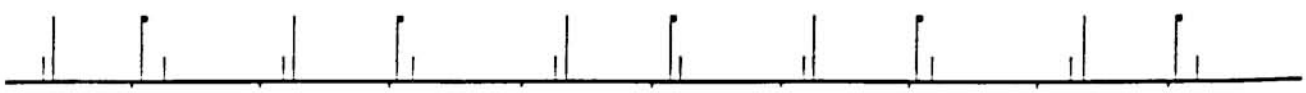

(b)

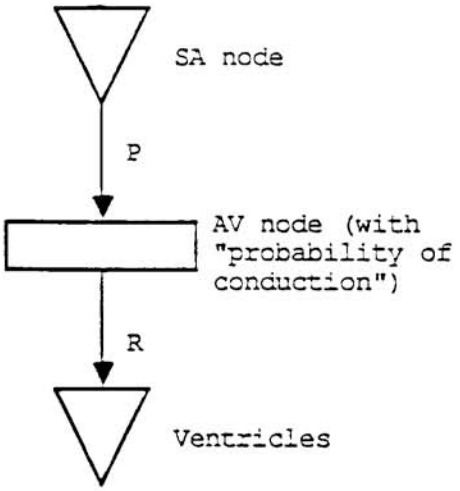

(a)

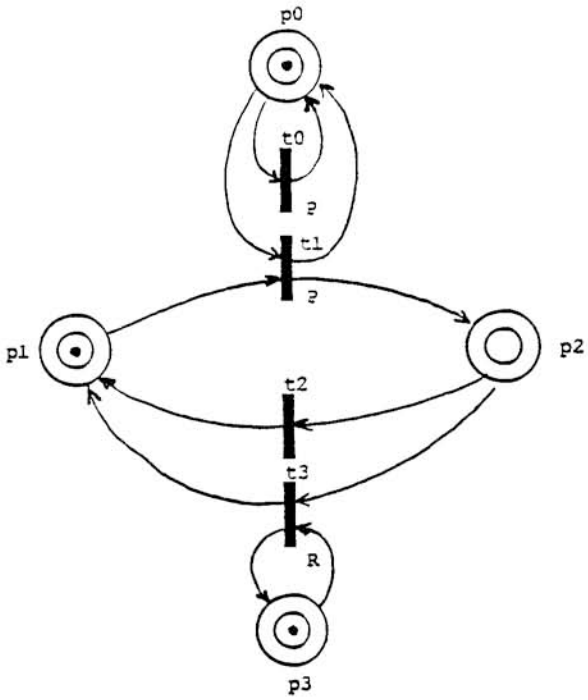

(c)

Second Degree AV Block

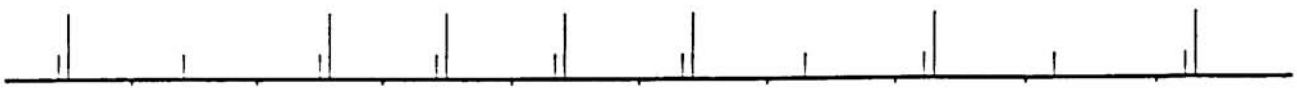

(b)

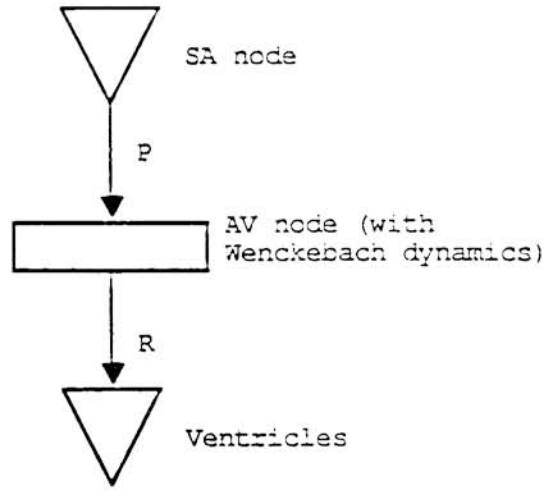
SA node
P
AV node (with
Wenckebach dynamics)
R
Ventricles

(a)

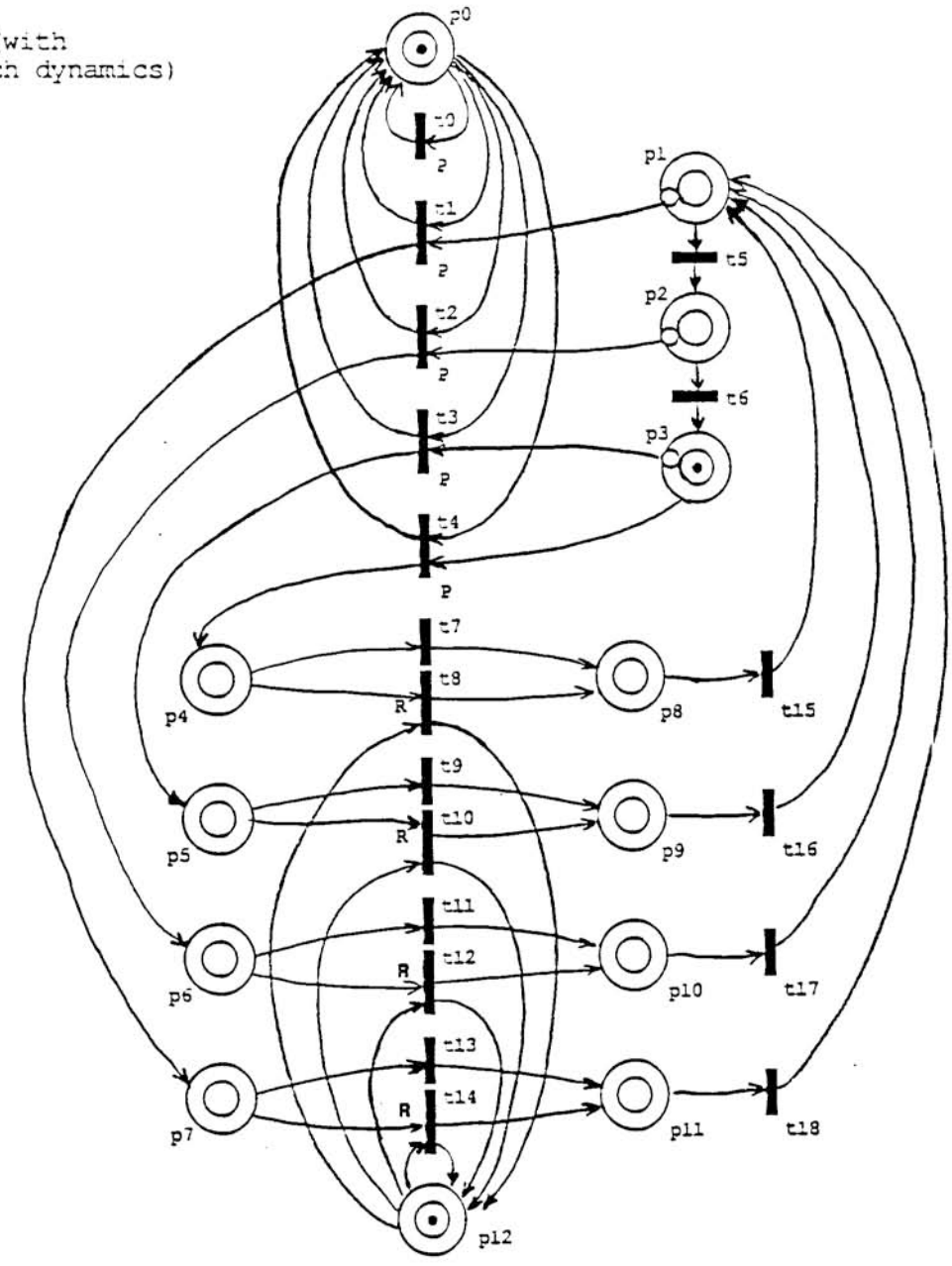
p0
t0
P
p1
t1
P
t5
p2
t2
P
t6
t3
p3
P
t4
P
t7
t8
R
p4
p8
t15
t9
t10
R
p5
p9
t16
t11
t12
R
p6
p10
t17
t13
t14
R
p7
p11
t18
p12

(c)

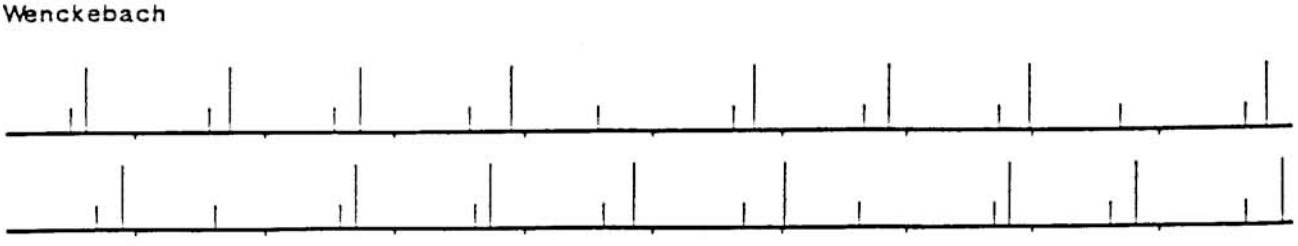
Wenckebach

(b)

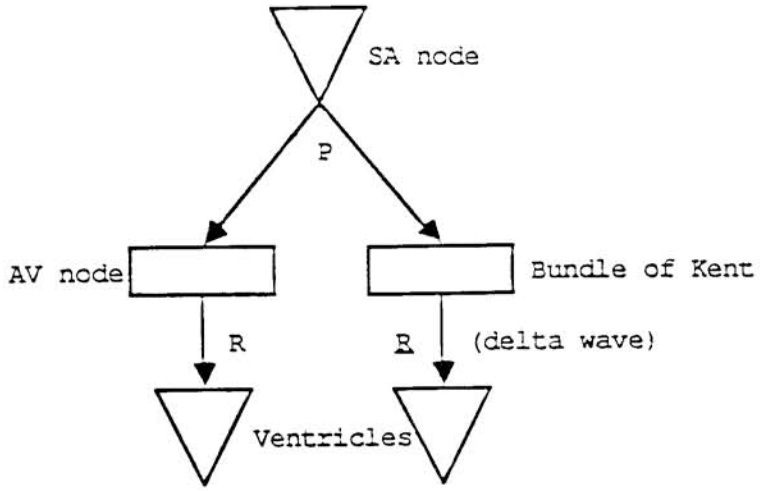

(a)

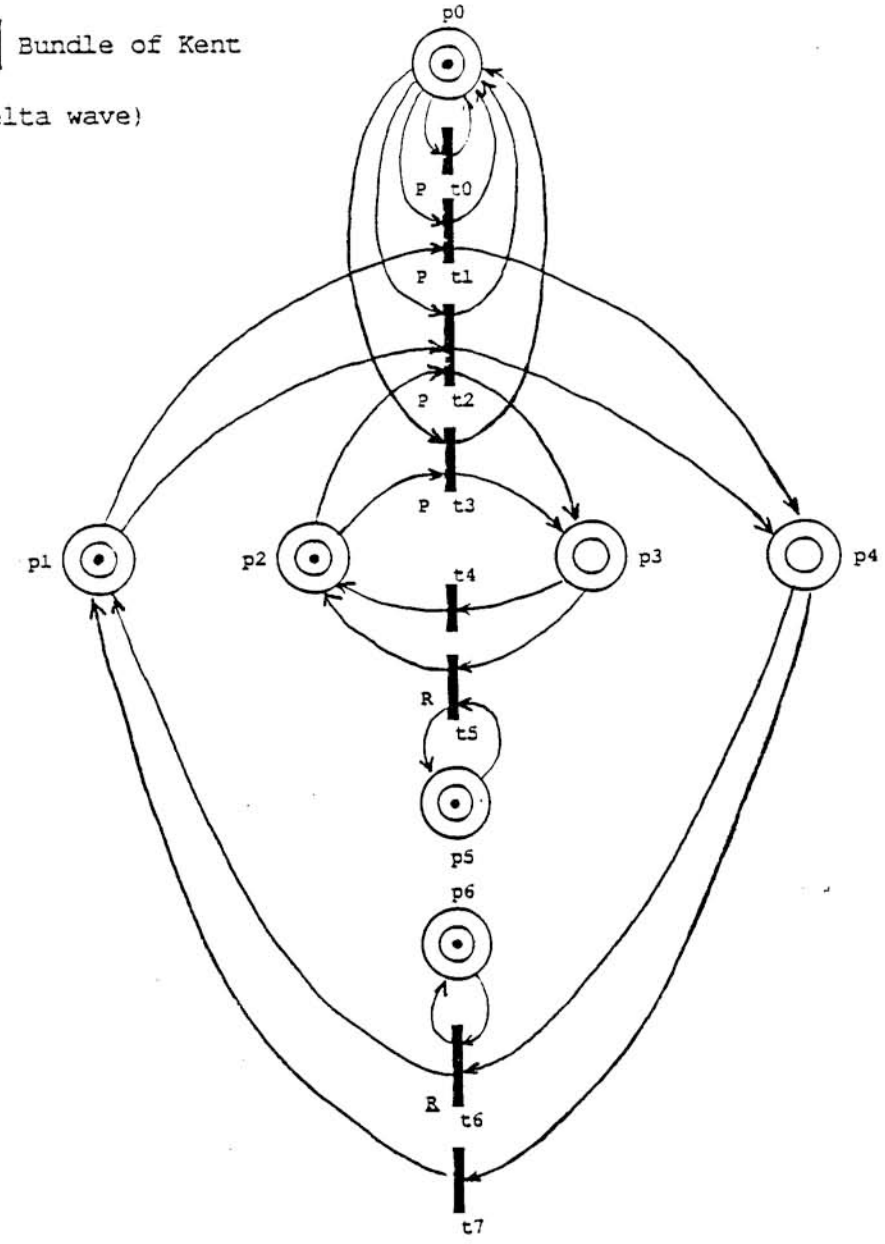

(c)

Wolfe-Parkinson-White

(b)

Figure 9

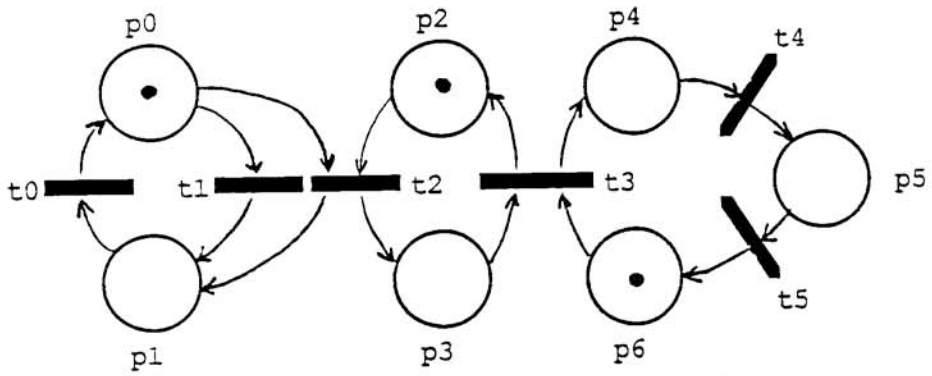

Figure 10

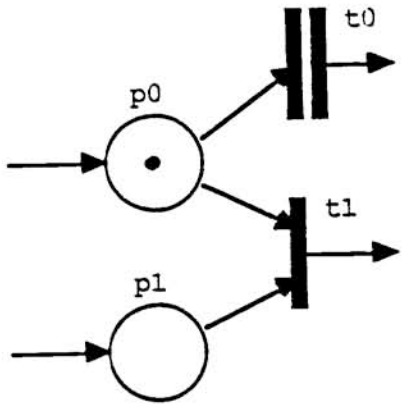

Figure 11

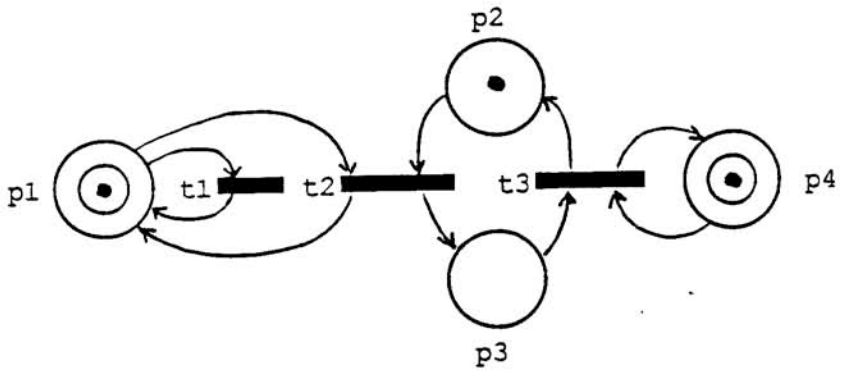

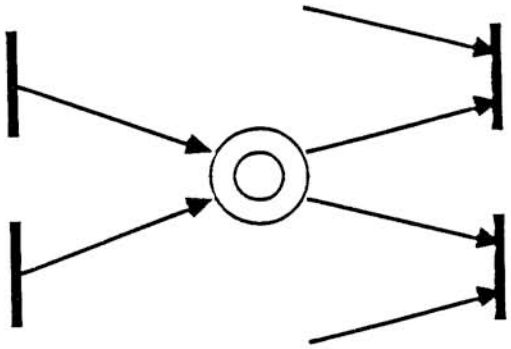

(a)

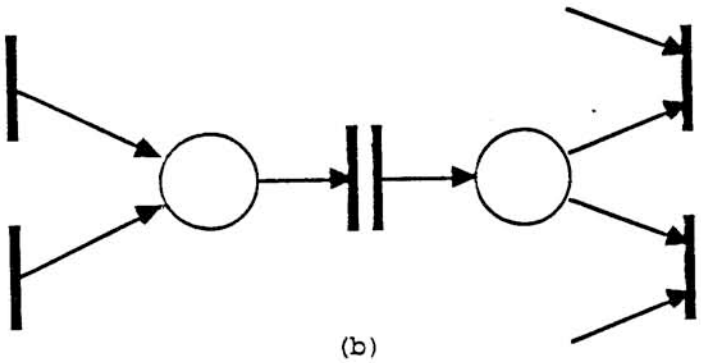

(b)

Figure 13

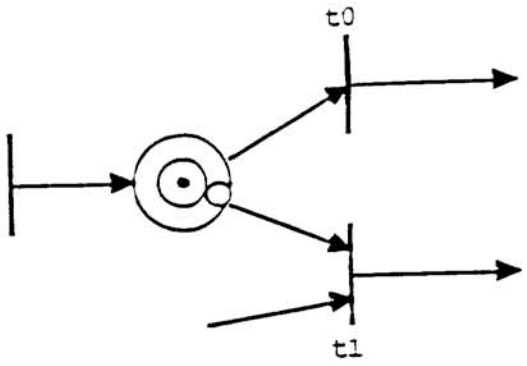

(a)

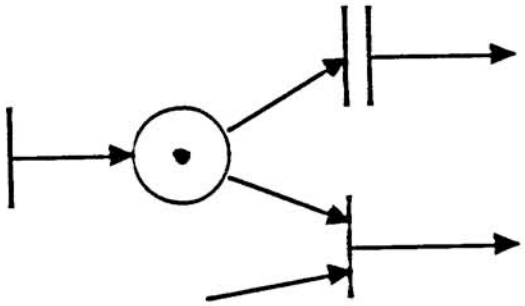

(b)

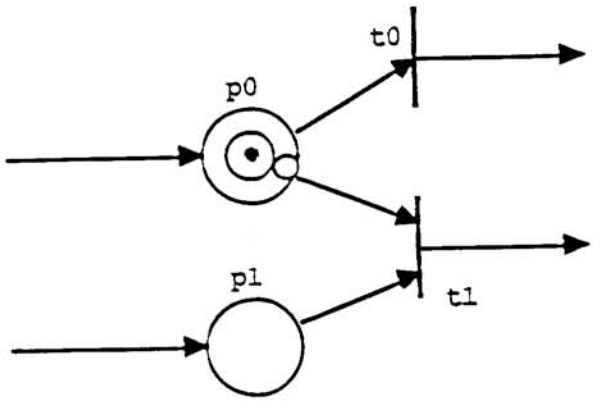

(c)

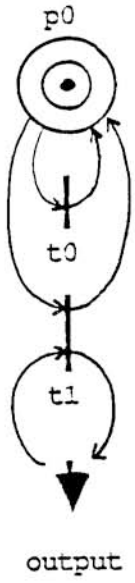

(a) Autorhythmic Unit

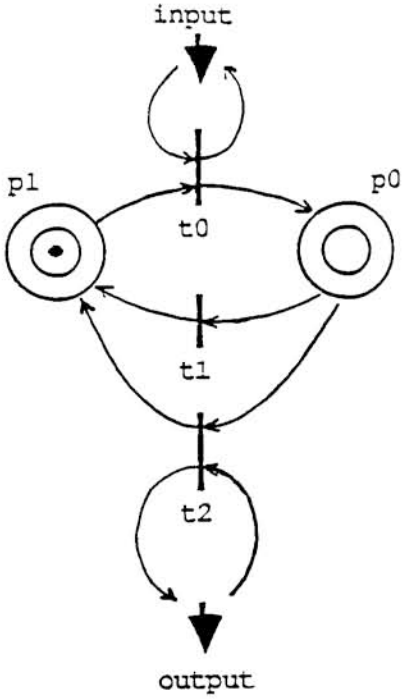

(b) Conduction Unit

(c) Absolute Refractory Unit

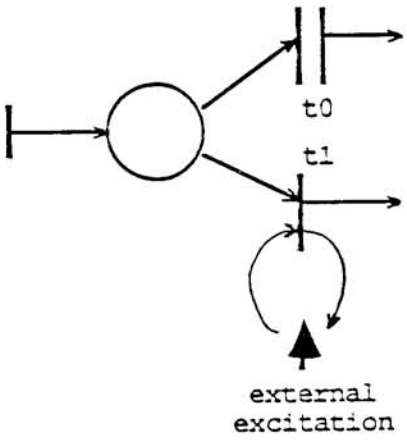

(d-1) Relative Refractory Unit "transition-timed" format

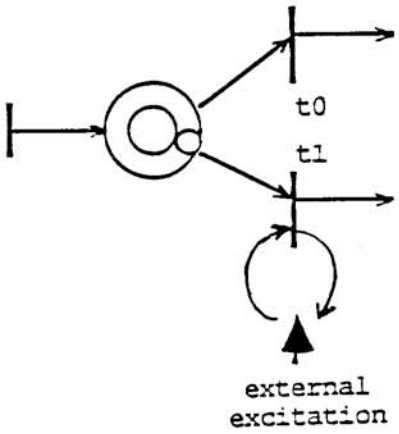

(d-2) Relative Refractory Unit "modified place-timed" format

Figure 15

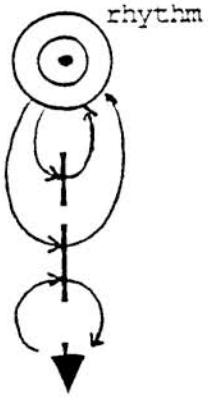

(a) Pacemaker

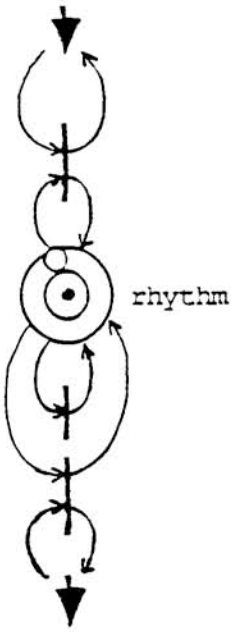

(b) Resettable Pacemaker

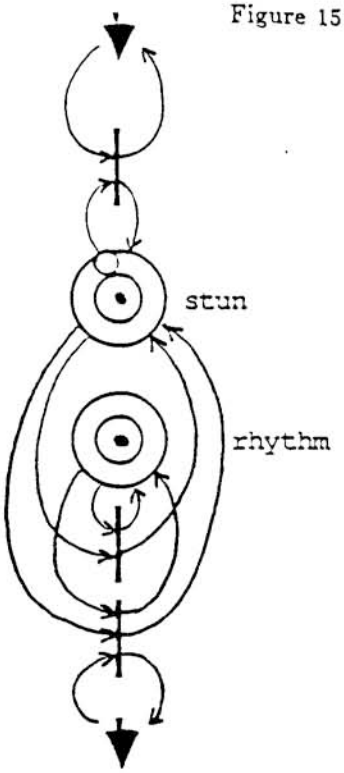

(c) Stunnable Pacemaker

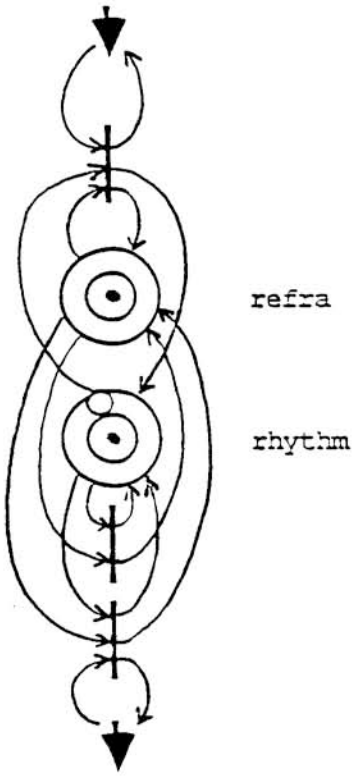

(d) Resettable Pacemaker with absolute refractory period

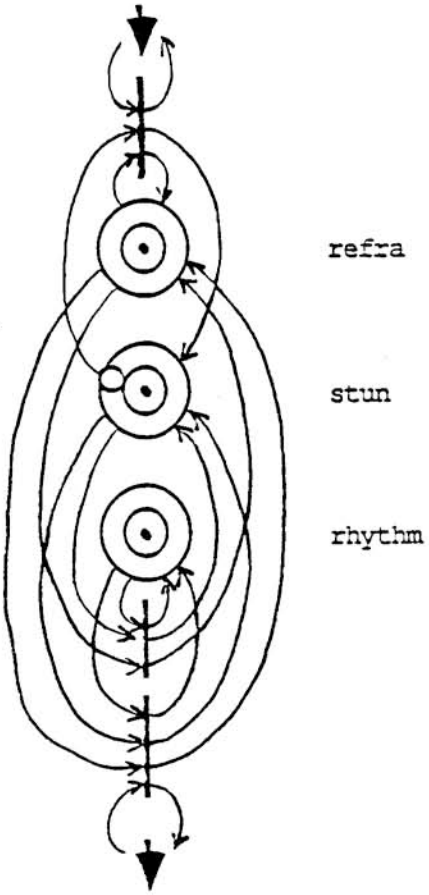

(e) Stunnable Pacemaker with absolute refractory period

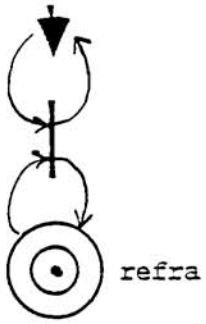

(f) Terminal

Figure 16

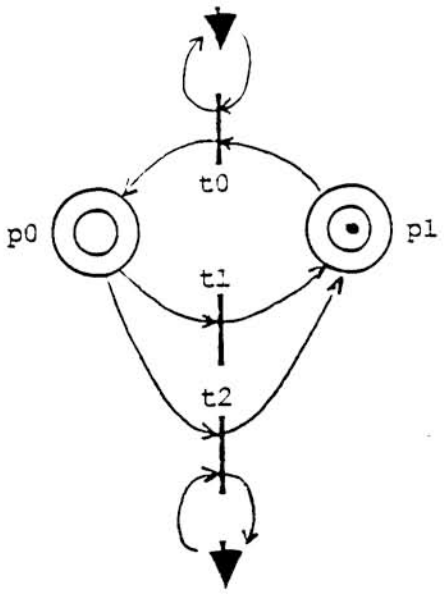

(a)

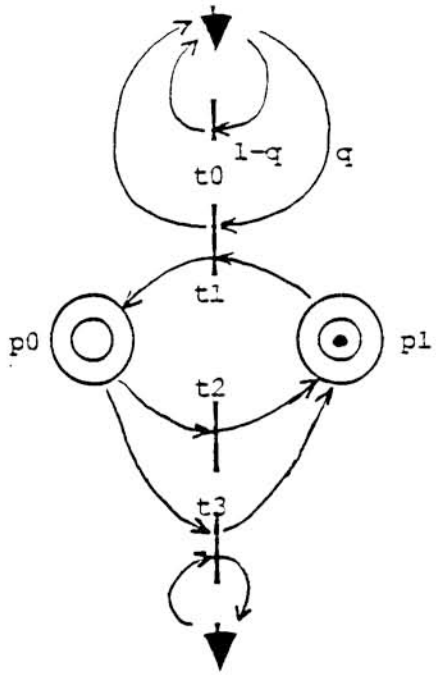

(b)

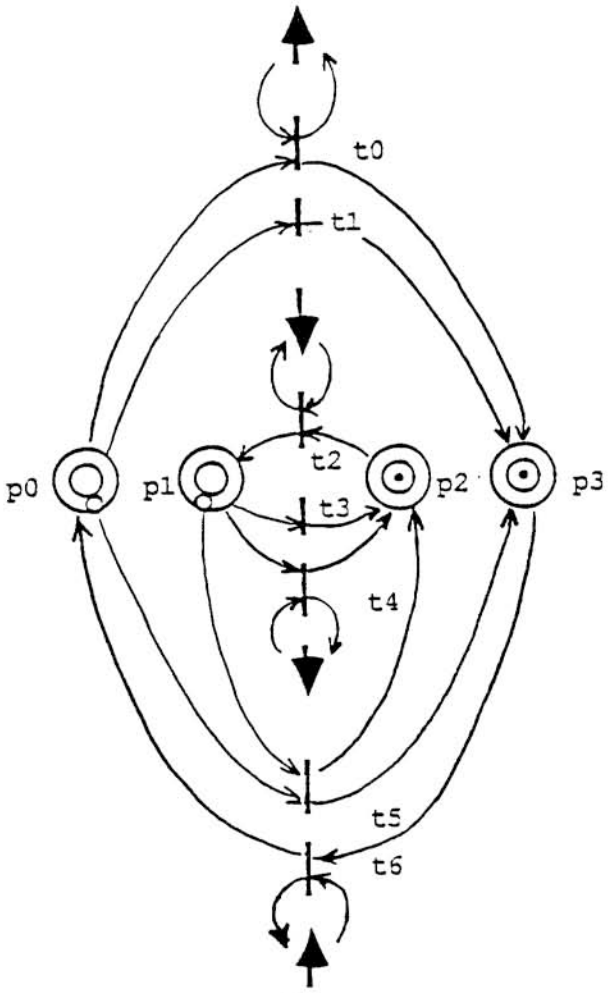

(c)

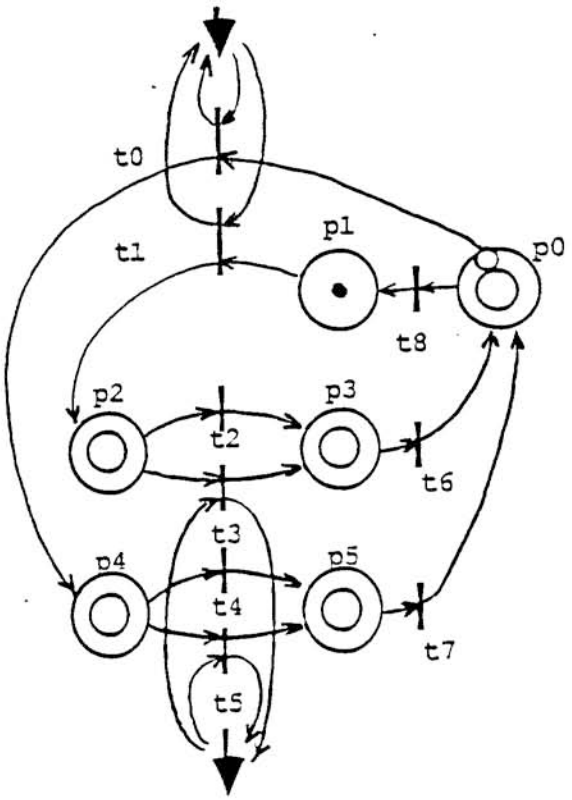

(d)

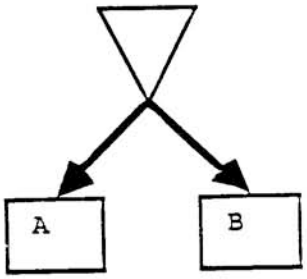

(a)

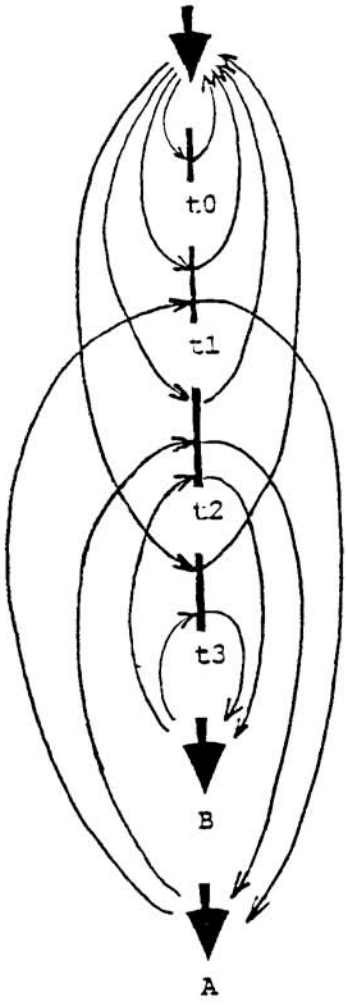

(b)

Figure 18

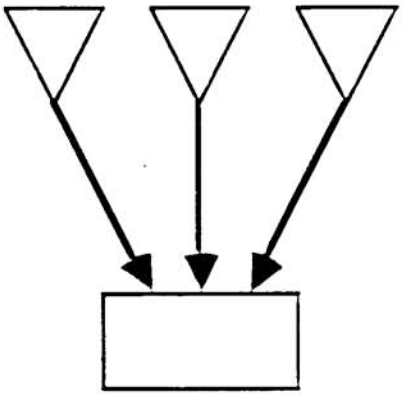

(a)

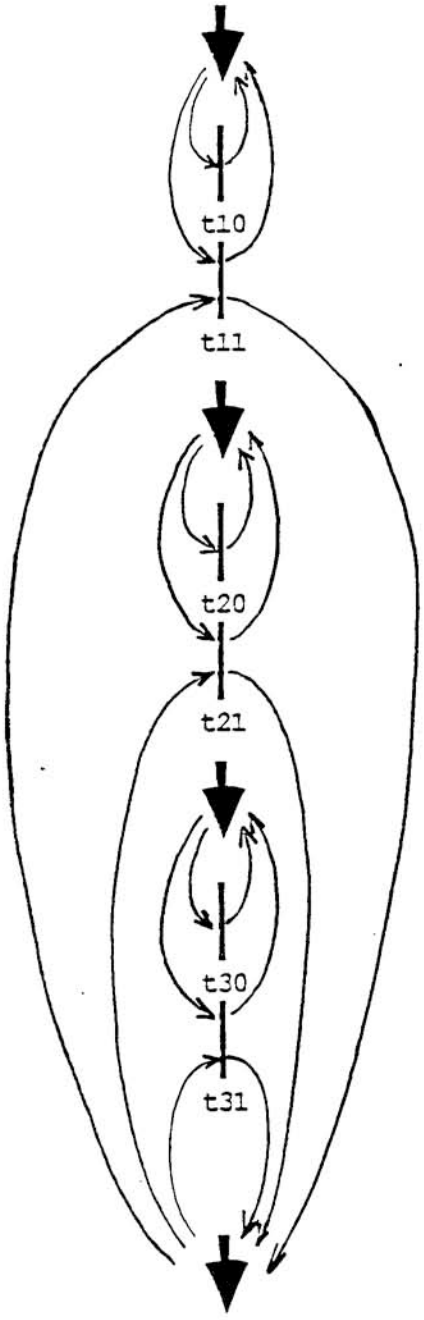

(b)

Table 1: Model Parameters

Normal Heart (Fig. 2c)

p0 (SA rhythm)	{ 0.92, 0.96, 1.00, 1.04, 1.08 }
p1 (AV refractory period)	{ 0.3 }
p2 (AV conduction delay)	{ 0.08, 0.10 }
p3 (Vent. refractory period)	{ 0.3 }

Atrial Premature Beat (Fig. 3c)

p0 (ectopic rhythm)	{ 0.6, 0.8, 1.5 }*

*non-uniform distribution: Prob(0.6) = Prob(0.8) = 0.15; Prob(1.5) = 0.70.

p1 (SA rhythm)	{ 0.92, 0.96, 1.00, 1.04, 1.08 }
p2 (AV refractory period)	{ 0.3 }
p3 (AV conduction delay)	{ 0.08, 0.10 }
p4 (Vent. refractory period)	{ 0.3 }

(continued to the next page)

Ventricular Premature Beat (Fig. 4c)

p0 (SA refractory period)	{ 0.3 }
p1 (SA rhythm)	{ 0.92, 0.96, 1.00, 1.04, 1.08 }
p2 (retrograde conduction delay)	{ 0.14, 0.16 }
p3 (AV conduction delay)	{ 0.08, 0.10 }
p4 (AV refractory - normal)	{ 0.3 }
p5 (AV refractory - retrograde)	{ 0.3 }
p6 (Ventricles refractory)	{ 0.3 }
p7 (ectopic rhythm)	{ 0.6, 0.8, 1.5 }*

*non-uniform distribution: Prob(0.6) = Prob(0.8) = 0.15; Prob(1.5) = 0.70.

Bigeminy (Fig. 5c)

p0 (SA rhythm)	{ 0.92, 0.96, 1.00, 1.04, 1.08 }
p1 (AV refractory period)	{ 0.3 }
p2 (AV conduction delay)	{ 0.08, 0.10 }
p3 (reentrant conduction delay)	{ 0.7, 0.8 }
p4 (Vent. refractory period)	{ 0.5 }
p5 (reentrant refractory period)	{ 0 }

(continued to the next page)

Second Degree AV Block (Fig. 6c)

p0 (SA rhythm)	{ 0.92, 0.96, 1.00, 1.04, 1.08 }
p1 (AV refractory period)	{ 0.3 }
p2 (AV conduction delay)	{ 0.08, 0.10 }
p3 (Vent. refractory period)	{ 0.3 }
Decision Rule for { t0, t1 }	Prob(t0) = 0.25; Prob(t1)=0.75.

Wenckebach (Fig. 7c)

p0 (SA rhythm)	{ 0.92, 0.96, 1.00, 1.04, 1.08 }
p1 (AV relative ref. sub-period)	{ 0.16 }
p2 (AV relative ref. sub-period)	{ 0.16 }
p3 (AV relative ref. sub-period)	{ 0.16 }
p4 (AV conduction delay)	{ 0.16, 0.20 }
p5 (AV conduction delay)	{ 0.20, 0.24 }
p6 (AV conduction delay)	{ 0.24, 0.28 }
p7 (AV conduction delay)	{ 0.28, 0.32 }
p8 (AV absolute refractory)	{ 0.48 }
p9 (AV absolute refractory)	{ 0.56 }
p10 (AV absolute refractory)	{ 0.68 }
p11 (AV absolute refractory)	{ 0.80 }
p12 (Vent. absolute refractory)	{ 0.28, 0.32, 0.36 }

(continued to the next page)

Table 1

Wolfe-Parkinson-White (Fig. 8c)

p0 (SA rhythm)	{ 0.92, 0.96, 1.00, 1.04, 1.08 }
p1 (Bundle Kent refractory)	{ 0.3 }
p2 (AV refractory)	{ 0.3 }
p3 (AV conduction delay)	{ 0.12, 0.14 }
p4 (Bundle Kent conduction delay)	{ 0.08, 0.10 }
p5 (Vent. refractory period)	{ 0.3 }
p6 (Vent. refractory period)	{ 0.3 }